EFFECTS OF NON-UNIFORMITY ON TROUGH INSTABILITY IN NONWOVENS

By

PHANIDHAR CHILUKA

Bachelor of Technology in Mechanical Engineering
Osmania University
Hyderabad, Telangana
2015

Submitted to the Faculty of the
Graduate College of the
Oklahoma State University
in partial fulfillment of
the requirements for
the Degree of
MASTER OF SCIENCE
December, 2018

EFFECTS OF NON-UNIFORMITY ON TROUGH

INSTABILITY IN NONWOVENS

Thesis Approved:

Dr. Shuodao Wang

Thesis Adviser

Dr. James K. Good

Dr. Karl Reid

ACKNOWLEDGEMENTS

I would like to thank my graduate advisor Dr. Shuodao Wang for his extensive support and guidance throughout my research. His patience and support have helped me to progress in my research. I would also like to thank Dr. Shuodao Wang and Dr. Good for giving me an opportunity to be a part of Web Handling Research Centre.

I would like to thank my committee members Dr. Good and Dr. Karl Reid for their advice. My special thanks to Ron Markum for his support throughout my research. He helped me in experimental setup and helped in LabVIEW programming. I would like to thank the WHRC sponsor for supporting my research.

I would like to thank my parents Muralidhar Chiluka and Padma Chiluka and my elder brother Shashidhar Chiluka for believing in me and supporting throughout my education.

Acknowledgements reflect the views of the author and are not endorsed by committee members or Oklahoma State University.

Name: PHANIDHAR CHILUKA

Date of Degree: DECEMBER, 2018

Title of Study: EFFECTS OF NONUNIFORMITY ON TROUGH INSTABILITY IN NONWOVENS

Major Field: MECHANICAL AND AEROSPACE ENGINEERING

Abstract:

A web is defined as a material whose length is very large compared to its width and the width is much greater than the thickness. Web material includes paper, fabric, metal, plastic film and composites. Nonwoven fabric is a fabric-like material made from long fibers that are bonded together by chemical, mechanical, heat or solvent treatment. In nonwovens, there exists thickness and modulus variations in many different regions over a length of web. In our research, we study on SMS nonwoven web. SMS refers to Spunbond-Meltblown-Spunbond which is a tri-laminate nonwoven web. Generally, web instability occurs between the rollers in the form of troughs and on the rollers in the form of wrinkles. The direction in which the web travels is called the Machine Direction (MD) and the direction perpendicular to the MD is called the Cross-Machine Direction (CMD). These instabilities can affect the web quality. Nonwovens have thickness and modulus variation in different regions in a span of web. Nonwovens are much more prone to the web instability than the uniform web.

Understanding the effects of non-uniformity is needed to solve trough/wrinkling problems in nonwovens. To understand the localized instability problems associated with nonwovens, two major challenges remain: (1) how to characterize the non-uniformity of nonwovens and how to relate the non-uniformity to the thickness and material property variations, and (2) how to implement the thickness and modulus variations in FEA to simulate troughs if the information in the previous step is obtained. This research is designed to answer these questions. Here, the thickness is correlated with the modulus (MD and CD directions). This is achieved by performing experiments to characterize the thickness distribution in nonwovens, characterizing effective material properties for web samples of different thickness, and adopt finite element analysis by considering material as isotropic and orthotropic to find out how the variation in material properties and thickness is related to trough instability, and then compare the FEA predictions to experimental results on critical troughing load and trough profiles.

TABLE OF CONTENTS

Chapter Page

LIST OF TABLES

Table Page

LIST OF FIGURES

Figure Page

Figure Page

CHAPTER I

INTRODUCTION

INTRODUCTION TO WEBS:

A web is defined as a material whose length is very large compared to its width and its width much greater than its thickness. Web material includes paper, fabric, metal, composites. Web processing operation includes printing, laminating, coating and converting into the final product where the final continuous web is cut into appropriate size. Web handling is a process where the web is transported continuously between the rollers. The main purpose of web handling is to transport this web through machines without affecting its properties.

NONWOVEN WEBS:

Nonwoven webs are the web structures formed by using mechanical, chemical, or heat treatment for bonding fibers. In general, the nonwovens are not made by weaving or knitting. They provide specific properties like liquid repellent, strength, absorbent, tear resistant etc. Nonwoven webs can be manufactured by using different fibers, different bonding agents which are suitable for the material and by using different processes.

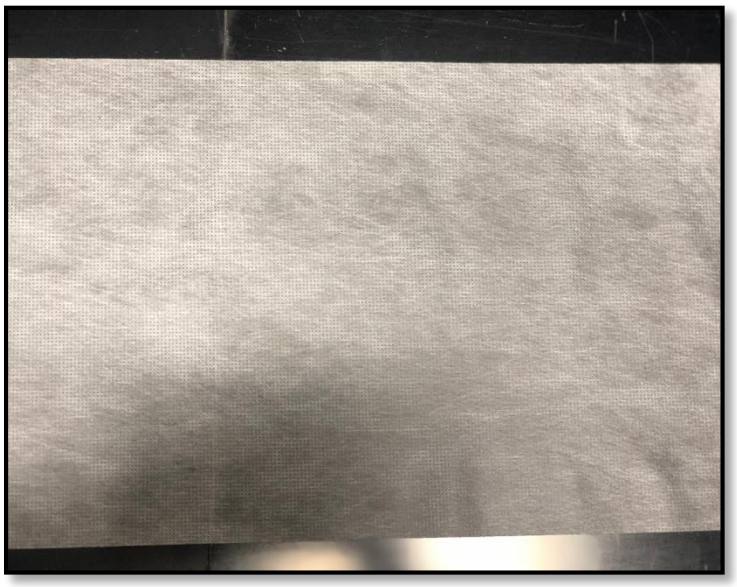

Figure 1.1: SMS Nonwoven fabric

Some nonwoven webs are manufactured by laminating two or more layers of nonwoven fabric which combines the properties of the layers used in the manufacture of the web. Generally, the nonwovens are produced by two methods i.e., dry method and the wet method. The nonwoven fabrics are useful in the application of medical, clothing, shoes and leather good, textiles for the home etc.

In our research, we study on SMS nonwoven web shown in Figure 1.1. SMS refers to Spunbond/Meltblown/Spunbond. It consists of a layer of meltblown (MB) fibers sandwiched between the two spunbond (SB) layers of polypropylene and polyethylene. In spunbond technology, polymer is extruded to form filaments of diameter ranging from 15-35 microns. Spunbond fibers has high liquid retention capacity and are heavier and stiffer than the MB fibers. In meltblown technology, melt blowing process is carried out to form fine fibers of diameter ranging from 2-4 micrometer. It is widely used in the medical and health industry, advertising and digital printing.

WEB INSTABILITY:

Web instability usually occurs when the web travels through the process machine on the rollers. The direction in which the web travels is called the Machine Direction (MD) and the direction perpendicular to the MD is called the Cross-Machine Direction (CMD). During web processing the web travel through the roller with an applied tension. Required tension to be applied to make the web as flat as possible for different web processing operations.

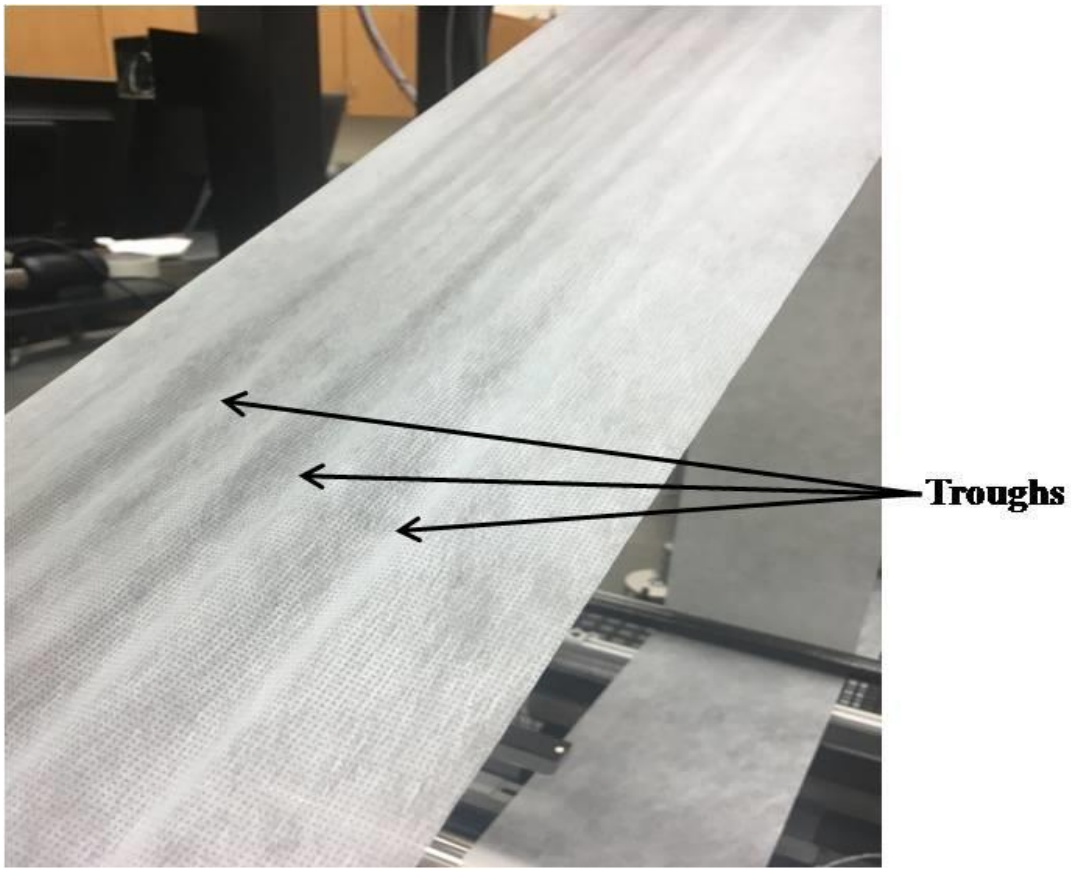

Figure 1.2: Trough instability [2]

Generally, web instability occurs between the rollers in the form of troughs as shown in Figure 1.2 and on the rollers in the form of wrinkles. Troughs often occur with or without wrinkles in the web processing. These instabilities can affect the web quality. We have previous studies on

web instabilities due to tapered roller and misaligned roller [4], [9]. For nonwovens combined thickness and modulus variation exist in different regions in a span of web.

RESEARCH OBJECTIVE:

The objective of this research is to experimentally characterize the non-uniformity in the nonwovens and analyze the trough formation in nonwovens by FEA that utilize the measured data. FEA predictions will be validated by the experimental results on critical troughing loads and trough profiles. In this research, variation of thickness and modulus are considered in nonwovens. The trough instability associated with nonwovens can be understood by pursuing the following specific aims:

(1) Determine experimental approach to characterize the thickness distribution in nonwoven webs: An ultrasound scanning method is used to determine the thickness distribution of a nonwoven sample. It provides a non-destructive experimental method to find the local mass density of the material.

(2) Establish the correlation between local thickness and effective modulus in different regions of a nonwoven: The web is divided into specific grid sizes and the average thickness of each grid is calculated. Then the samples of respective thickness are cut from the web to perform experimental tests in order to find the modulus for respective thickness.

(3) Apply the effective property map from Step 2 in finite element simulations to predict troughs. Compare the simulated result with static experimental testing: Here, experiments will be conducted under clamped loaded ends in the MD and free edges in the CMD to obtain the critical troughing loads and the post-buckling trough profiles.

CHAPTER II

LITERATURE REVIEW

BENDING STIFFNESS OF PAPERBOARDS:

Testing standard "T 535 om-96" [1] determined the bending stiffness of paper and paperboard (resonance length method). It was mentioned that this test can be performed for materials having low grammage. This test method assumes that there exists a correlation between the resonance length of a vibrating test strip of paper and its bending stiffness. A test specimen is clamped at one end, and the clamp is vibrated at a specified frequency and the resonance length of the specimen is measured. Based on the obtained resonance length and weight of the material the bending stiffness can be calculated.

The bending stiffness S^b of the material is determined by the expression:

$$S^b = \frac{4\pi^2}{k^4} \, l^4 w' f^2 \times 10^{-12} \qquad (2.1)$$

where l is the resonance length of a rectangular sample in mm, w' is the grammage in g/m^2, f is the vibration frequency (constant value: 25 Hz) and k is the dimensionless constant which is equal to 1.875 for the fundamental frequency of oscillation.

AMPLITUDE AND WAVELENGTH OF TROUGHS IN ORTHOTROPIC WEBS:

Nukala [2] derived the equation for amplitude of troughs in orthotropic web. In this paper, it was assumed that the principal modulus E_x and E_y are considered. In Figure 2.1, σ_x and σ_x shown acting on the plane as assumed by Timoshenko [6].

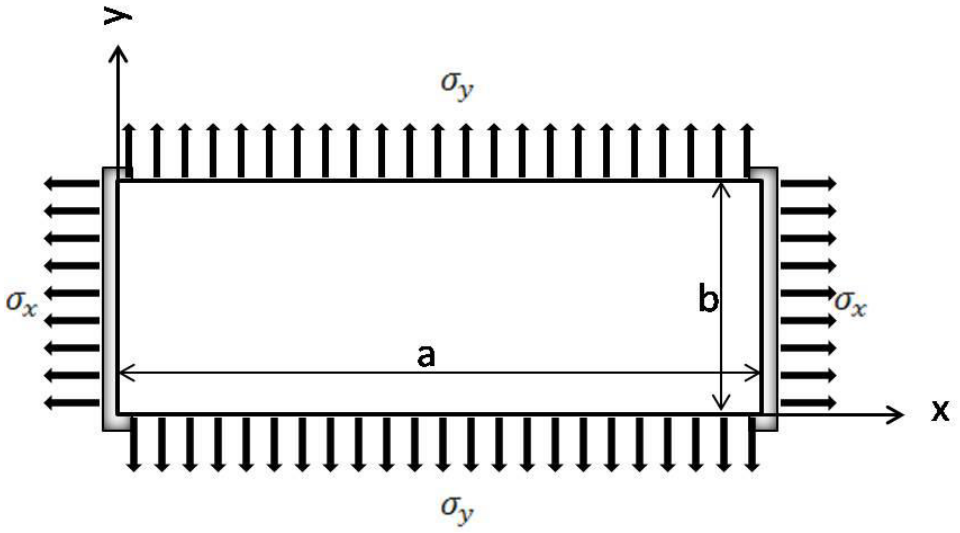

Figure 2.1: **Rectangular plate under biaxial stress with simply supported edges**

The expression for amplitude of troughs on orthotropic webs is derived by using the "Condition of Inextensibility" [12]. The derived amplitude was compared with the experimental and finite element results. The "Condition of Inextensibility" [2], [12] is described as the reduced width due to out of plane displacement is equal to the reduced with due to Poisson's effect.

The reduced width due to out of plane displacement is expressed as,

$$\int_0^b \left(1 - \frac{1}{2}\left(\frac{\partial \omega}{\partial y}\right)^2\right) dy = b' \qquad (2.2)$$

The reduced width due to poisons ratio is expressed as,

$$\int_0^b \left(1 - \frac{\nu_{xy}\sigma_x}{e_n}\right) dy = b' \tag{3.3}$$

By equating the two equations (2.2) and (2.3) due to different effects, it is defined as,

$$\int_0^b \left(\frac{1}{2}\left(\frac{\partial \omega}{\partial y}\right)^2 - \frac{\nu_{xy}\sigma_x}{e_n}\right) dy = 0 \tag{4.4}$$

By integrating the second term, the equation is simplified as follows,

$$\int_0^b \frac{1}{2}\left(\frac{\partial w}{\partial y}\right)^2 \cdot dy = \frac{2b\,\nu_{xy}\sigma_x}{E_x} \tag{2.5}$$

The out of plane displacement equation given by equation below is substituted in the above equation to derive the amplitude [3].

$$w(x,y) = A_{mn} \sin\left(\frac{m\pi x}{a}\right) \sin\left(\frac{n\pi y}{b}\right) \tag{2.6}$$

After substituting, the amplitude is given by,

$$A = \left[\frac{\left(\frac{2b\,\nu_{xy}\,\nu_X}{e_x}\right)}{\frac{b}{2}\left(\frac{n\pi}{b}\right)^2}\right]^{\frac{1}{2}} \tag{2.7}$$

where n is [12],

$$n = \sqrt{\frac{2}{\pi a t}}\left[\frac{3\left(1 - \nu_{yx}\,\nu_{xy}\right)\sigma_x}{E_y}\right]^{\frac{1}{4}} b \tag{2.8}$$

By eliminating the smaller order terms, we get the final expression for amplitude as [2],

$$A = \sqrt{\frac{2at\,\nu_{yx}}{\pi}}\left(\frac{\frac{\sigma_x}{E_y}}{3\left(1-\nu_{yx}\,\nu_{xy}\right)}\right)^{\frac{1}{4}} \tag{2.9}$$

The amplitude derived in equation (2.7) is compared with the finite element analysis and experimental results. The compared results are similar when they are compared with the finite element simulations.

The wavelength can be obtained by dividing total width of the web by number of troughs, i.e., dividing the width by equation (2.10) which is given by,

$$\lambda = \frac{b}{(2n)} = \frac{\sqrt{at\pi}}{(2\sqrt{2})\sqrt[4]{\frac{3\left(1-\nu_{yx}\,\nu_{xy}\right)\sigma_x}{E_y}}} \tag{2.10}$$

According to Good and Biesel's model [11] on trough formation, the critical CMD stress required to buckle the web is:

$$\sigma_{y,cr} = -\frac{\pi t}{\sqrt{3}a}\sqrt{\frac{\sigma_x\,E_y}{(1-\nu_{yx}\,\nu_{xy})}} \tag{2.11}$$

where, σ_x is the average MD stress, a is the span of the web in MD, E_y is the modulus in CMD, ν_{yx} and ν_{xy} are the poisson's ratio, t is the thickness of the material.

Maxwell's reciprocal theorem can be used to relate the Poisson's ratio and modulus,

$$\frac{\nu_{xy}}{E_x} = \frac{\nu_{yx}}{E_y} \tag{2.12}$$

Nukala [2] assumed constant thickness for orthotropic web and performed the finite element simulations. The simulations did not show any signs of buckling. The buckling was when the experiments are conducted and it was believed that the buckling is due to non-uniformity of the web thickness. It was also found that the profile of trough is not consistent when different samples are compared. It was believed that it is due to the variation of thickness in orthotropic web.

Mallya [8] performed the experimental method and finite element analysis to predict the wrinkles on a web due to circular voids and elliptical voids. It was found that the web instability is affected by the presence of voids. It has been shown that the wrinkles generated by the web with elliptical void is worse than the wrinkles generated by the circular void. In this research the effect of span length on wrinkling is not studied. The effect on wrinkling of webs due to voids like circular and elliptical is studied, but the effect on wrinkling of webs due to other shape voids can be studied, since these voids could be more complicated or less complicated than the voids studied in this research.

Baipa [7] performed finite element simulation to analyze the wrinkles on web with circular non-uniform regions. The effect of various parameters such as thickness, size of the non-uniformity, width of the web with non-uniform regions are analyzed. The thick and thin non-uniformities are compared to study the effect of size of non-uniformity. It has been found that the whether the has web has thicker or thinner non-uniformity, web instability was observed. It was found that the web whose non-uniformity is thicker buckle at higher tensions compared to the web with thinner non-uniformity. The web which has a large width wrinkled at higher tension compared to the web with small width in the case of thicker non-uniformity. Web with multiple non-uniformities were analyzed in this research.

CRITICAL STRESS TO INDUCE TROUGHS IN ISOTROPIC WEBS:

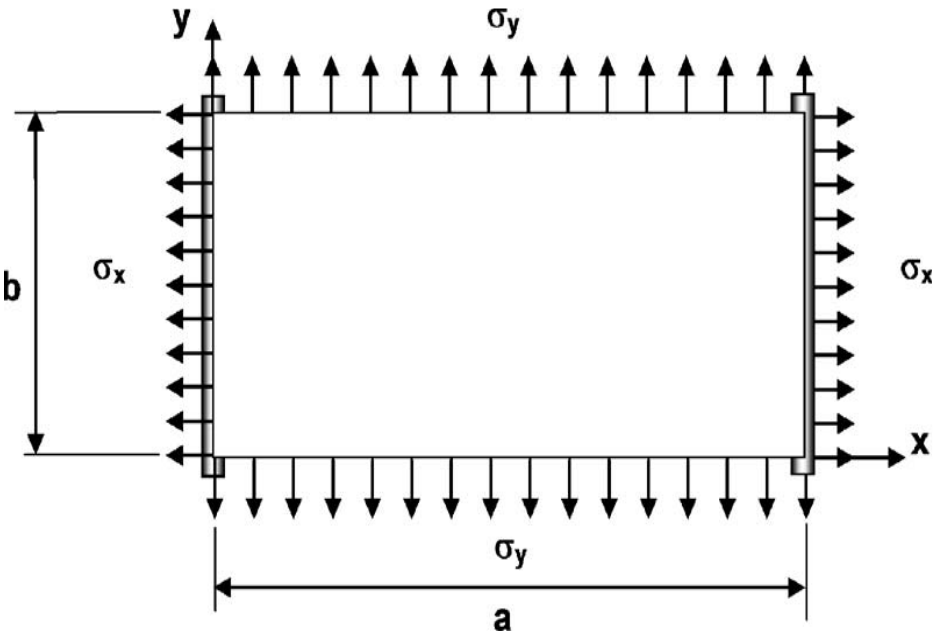

Figure 2.2: An isotropic web of span a between the rollers [3]

According to Good and Beisel's [3], [5] model on trough formation, the critical CMD stress for forming trough is:

$$\sigma_{y,cr} \approx -2\sqrt{\sigma_x \sigma_e + {\sigma_e}^2} + \sigma_e \tag{2.13}$$

where,

$$\sigma_e = \frac{\pi^2 D}{a^2 t} \tag{2.14}$$

and D is the CMD bending stiffness of the web.

The negative sign indicates that the σ_y stress is compressive in order to induce troughs. Good and beisel [5] calculated the σ_e by substituting the material properties, thickness and span of the web and found that the σ_e is very small compared to the σ_x. The equation (2.8) is simplified to

$$\sigma_{y,cr} \approx -2\sqrt{\sigma_x \sigma_e} \tag{2.16}$$

CHAPTER III

EXPERIMENTAL METHOD TO IDENTIFY THE DENSITY VARIATION AND MATERIAL PROPERTIES IN NONWOVEN WEBS

EXPERIMENTAL METHOD TO IDENTIFY THICKNESS VARIATION:

Observing a nonwoven sample from a human eye, we can see visual differences in different locations. The hypothesis here is that the density of fibers will affect the thickness and material properties of the web. A MeSys USM-200 scanner is used to obtain the thickness distribution of nonwoven web.

MESYS USM-200 SCANNER:

MeSys USM-200 scanner shown in Figure 3.1 is used to determine the weight and thickness of the thin materials. The thickness of the materials ranges from 0-800 μm. It is an ultrasonic absorption, non-contact, non-radiation scanner. Thin materials like paper, plastic and electrically conductive materials like aluminum, etc., can be measured by travelling across the material without contact.

Figure 3.1: MeSys USM-200 scanner

The measurement principle is based on local oscillation as shown in Figure 3.2. The transmitter (round spot diameter of 5 mm) transmits the wave through the material and the receiver reflects the wave. Due to the thickness variation in the material, the transmission and reflection of the oscillation varies.

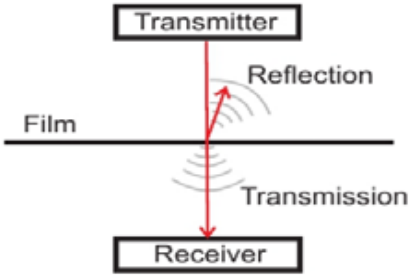

Figure 3.2: Measurement principle

EXPERIMENTAL SETUP:

The experimental setup shown in Figure 3.3 consists of MeSys USM-200 scanner, 2 clamps, 2 rectangular bars, 2 guides, 2 rails, data acquisition system (DAQ), a user interface to record the thickness variation of nonwoven web. The clamps, guides and rails used in this experiment are custom-made.

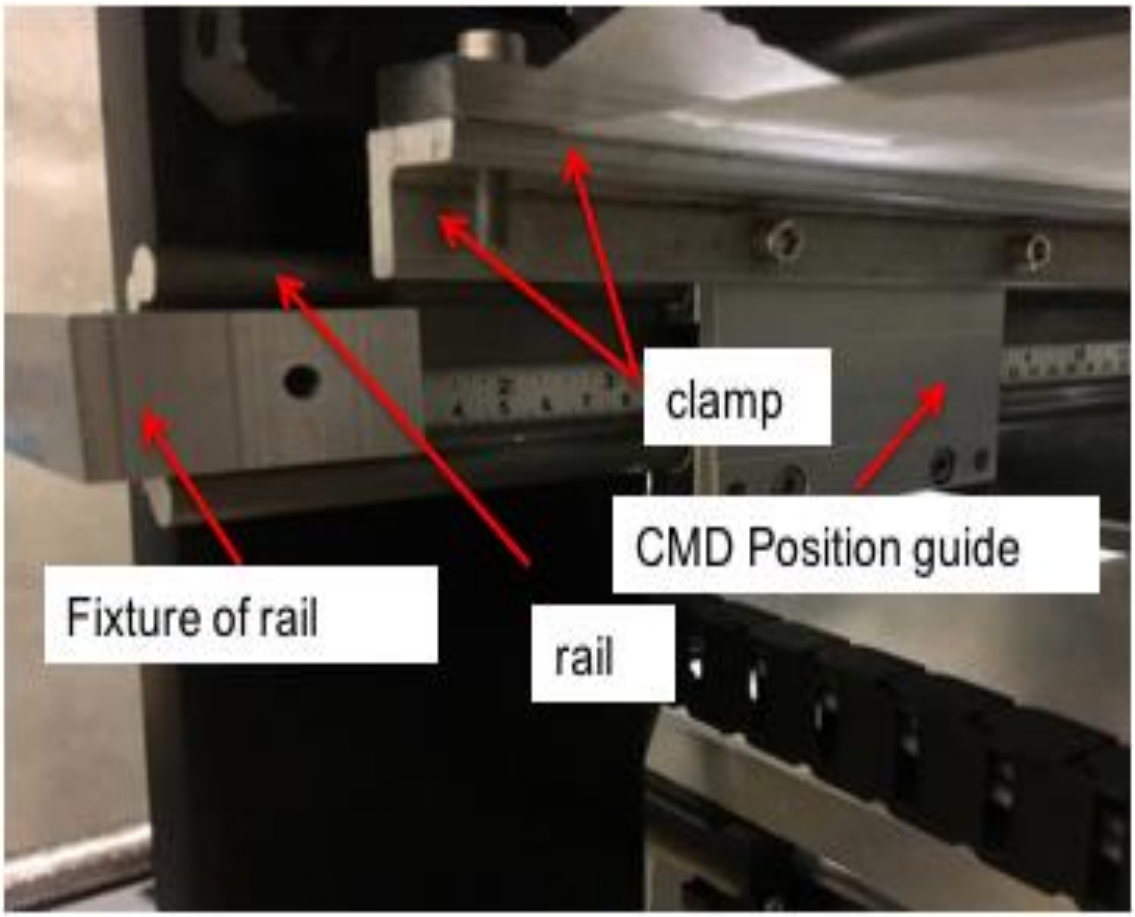

Figure 3.3: Experimental setup

Firstly, the clamps are designed in the solid works and are machined to the required size using the milling machine. The clamps, rail and guide are assembled in solid works before they are machined in order to ensure that these three parts fit perfectly. The clamp is used to hold the rail to the frame as shown in Figure 3.3 using screw knob. The rail is machined to the required length.

Then, the guide is fixed to the rail, which is clamped to the support using the clamp. The rectangular bars are fixed to the guide as shown in Figure 3.3. The rectangular bars are used to clamp one end of the web. The CMD guide move the web in CMD. The same procedure is repeated on the other end of the scanner to clamp the other end of the web. The rectangular bars should be in horizontal direction and it can be verified by using the leveling screw. The whole setup should be arranged in such a way that the web should pass through the midpoint of the transmitter and receiver when it is clamped on the two ends. The scanner is connected through DAQ to the user interface to record the thickness variation when the scanner moves along the web in MD. The thickness variation is recorded through DAQ using a LabVIEW program.

PROCEDURE:

The aluminum rectangular clamps were used to clamp the nonwoven web at two edges. The web should be clamped orthogonal to the clamps. The clamps should have good friction surface to avoid a slippage of the web. A double-sided tape is used to attach the web to the clamps. The clamps are mounted to the guide on each side using screws.

The scanner can be operated from the LabVIEW program. After initializing the scanner and placing the web between the clamps, the sample thickness (for example 4.77 mil [13]) value should be entered in another LabVIEW program and run the program. Now this is considered as the reference thickness value where the scanner is positioned on the web. The starting and ending position of the scanner should be entered. Then the scanner moves to and fro between the given distance. When the scanner starts to move along the MD, the thickness value changes depending on the variation in thickness of the nonwoven web. In this experiment, we use a web of 7.5 in width. The thickness distribution of web is recorded for an area of 23 in along length and 7 in along width. The scanner travel along the machine direction of the web and records the thickness value. The web is moved manually in the cross-machine direction for every 0.125 in along the width. The

thickness readings are recorded along the MD of the web at every point along the width in CMD. The thickness distribution is collected for a web span of 23×7 in.

NORMALIZING THE THICKNESS VALUE:

The MeSys measurement is dependent on the thickness of web at the starting scanning position. In order to obtain consistent readings from the scanner, different starting positions along the MD on a nonwoven web is marked as shown in the Figure 3.4 (a). The thickness at each point is measured 10 times by using the thickness gauge. The scanner starts the scanning at one point and the thickness at that point is entered as the initial thickness value in the program and the thickness distribution along the MD of the web is recorded. The same procedure is carried out by starting the scanning at different positions. The graph shown in Figure 3.4 (b) shows the thickness distribution in MD when starting at different locations. From the graph, it was found that the thickness variation profile is constant but the absolute values are dependent on the initial position thickness entered to the program. In order to get the consistent thickness readings for all the webs, the scanning starts at one point and a nominal thickness value of 4.77 mil [13] is entered. After the thickness value of the entire web is obtained as described in the next section, the average thickness of each web is normalized to the average value of 4.77 mil.

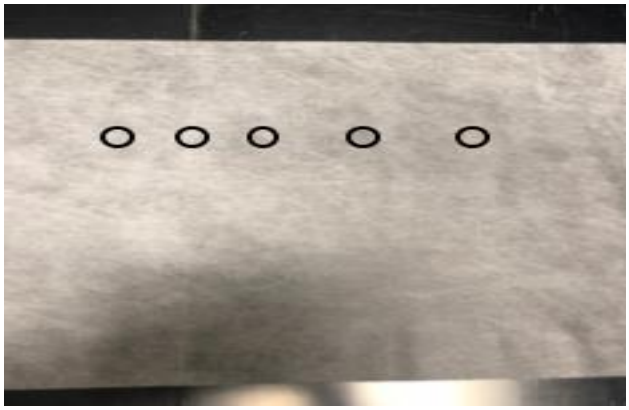

Figure 3.4: (a) Web marked at different spots along MD

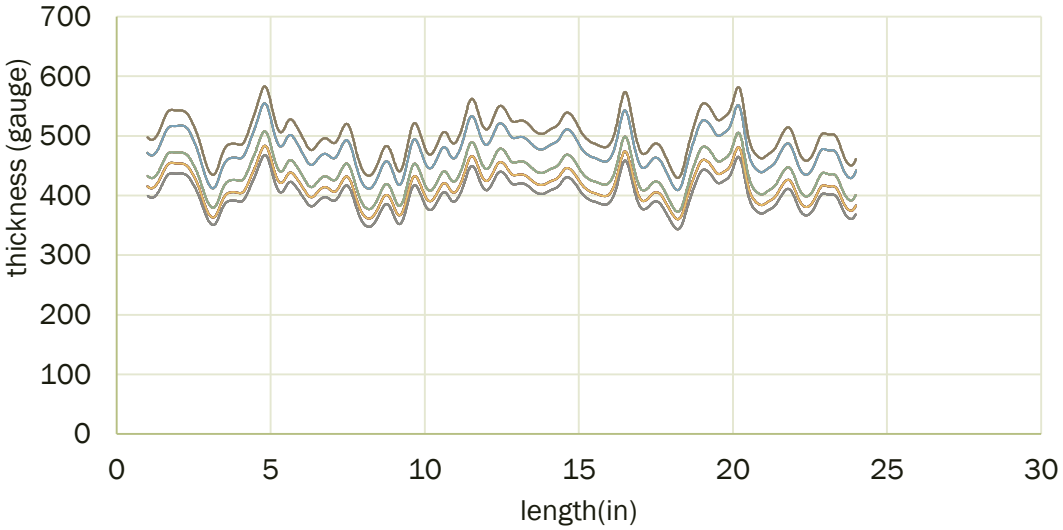

Figure 3.4: (b) Thickness distribution in the MD when starting at different locations

OBTAINING THICKNESS VALUES FOR THE ENTIRE WEB:

The scanning starts at a certain CMD position (near one of the longer edge of the web), and the scanning is programmed to travel along the entire MD span to collect the data that is spaced at 0.125 in. Each scan will provide the thickness values (similar to those in Figure 3.4 (b)) as a function of MD length for a given CMD position. The web is then moved every 0.125 in along the CMD, and the scanning is repeated for the next CMD position. The test is repeated until data sets for all the locations of the web are collected.

CALCULATING AVERAGE THICKNESS FOR APPROPRIATE GRID SIZE:

The thickness data is collected for a web of 23×7 in by the method described above. It is imported into excel file. The web area is divided into required grid size, for example, 1×0.5 in^2 and the average thickness of each grid is calculated. After calculating the average thickness of each grid, the thickness map of entire web is generated as shown in Figure 3.5 by using MATLAB code. The thickness map is used to show the variation of fiber thickness over entire web. The thickness map of nonwoven web of 23×7 in is shown in Figure 3.5.

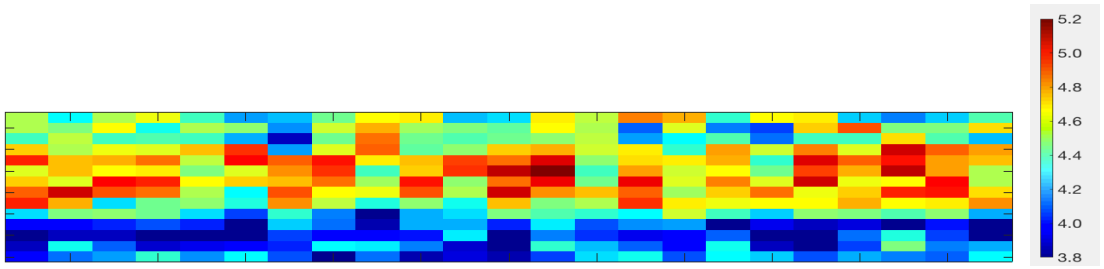

Figure 3.5: Thickness map of a nonwoven web of 23×7 in (unit: mil)

ESTABLISH CORRELATION BETWEEN LOCAL THICKNESS AND EFFECTIVE MD MODULUS IN DIFFERENT REGIONS OF NONWOVEN WEB:

From the thickness map, distinct local web region of different thickness can be determined. For example, we can find the 4.70 mil thickness samples on the thickness map. Different samples having the same local thickness value are collected from the scanned web. For example, grid size indicating 4.70 mil thickness value are collected and grid size having 4.70 mil thickness value are collected. The web is placed on the cutting mat as shown in the Figure 3.6. The web is divided into appropriate grid size by using the marker or pen to cut the samples of relevant thickness from the web as shown in Figure 3.7. Samples of relevant thickness are collected for each web. The same procedure is repeated to collect web samples of different thickness.

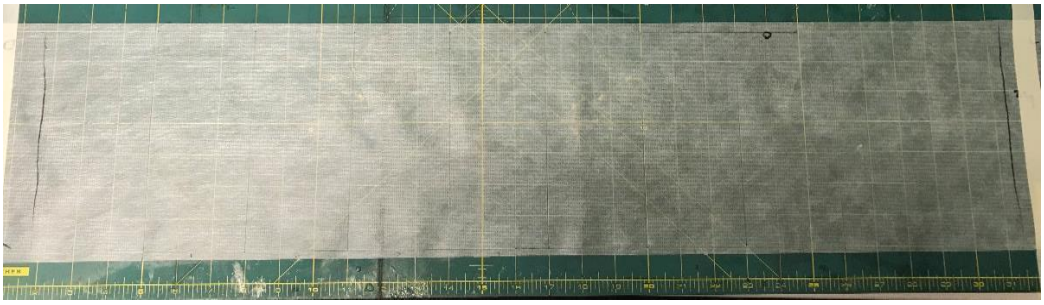

Figure 3.6: Web placed on the cutting mat

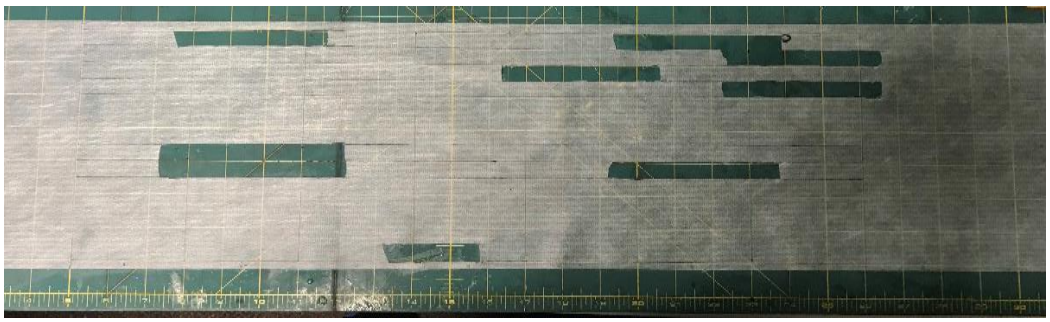

Figure 3.7: Web after collecting the sample

TENSILE TEST:

The Instron 5942 universal testing machine shown in Figure 3.8 is used for the static tensile test. The machine is specifically customized for ultra-low force measurements and will be suitable to test very small samples. It is customized for accurate force (±0.4% accuracy down to 0.05 N) and displacement (±0.1% accuracy down to 0.02 mm) measurements. The load versus displacement data is recorded for each sample. Assuming the material to be uniform within the local region, the relation between the measured force F and displacement U will be $F = EwtU/L$, where E is the effective MD Young's modulus, w is the width of the test specimen, L is the length of the sample and t is the effective thickness.

From the experiment, we can calculate the combined parameter ($EA = Ewt$) from the equation (2.8)

$$EA = \frac{FL}{U} \tag{3.1}$$

Figure 3.8: Instron machine

PROCEDURE:

After collecting the nonwoven samples of different thickness, each sample is tested to find the combined parameter value (EA). The nonwoven sample is placed between the two clamps as shown in Figure 3.9. The web sample should be placed in such a way that it should be orthogonal to the clamps. Clamping the web at a certain angle will affect the material property of the web. The clamps hold the sample tightly while performing the operation. The Instron machine comprises pneumatic clamps which use air actuated cylinders to operate the clamping action.

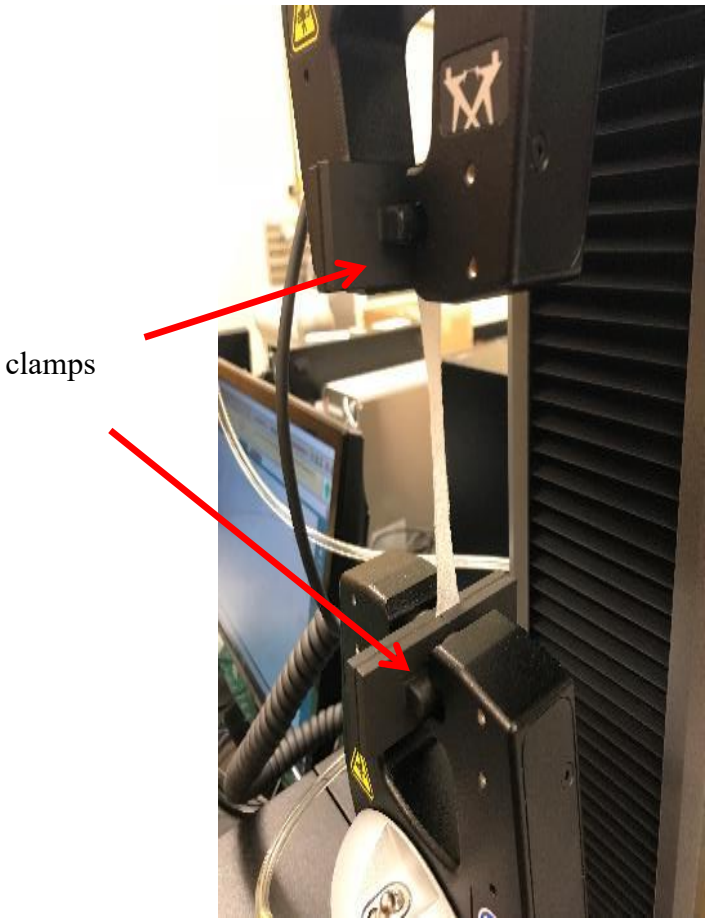

Figure 3.9: Nonwoven web clamped at both ends

The length L and width w of the sample should be measured before loading it on the machine. The BLUE HILL software is used to perform the tests on Instron machine and to export the output data in our required format. During testing, the tensile load is applied on the web sample at a constant rate and the load vs. displacement data is recorded. The load vs. displacement is exported into excel file. The load vs displacement graph is plotted from the data and the linear slope of the curve (F/U) is determined as shown in Figure 3.10. The slope value is substituted in equation (3.1) to obtain the EA value. The same procedure is to calculate the EA value for samples of different thickness.

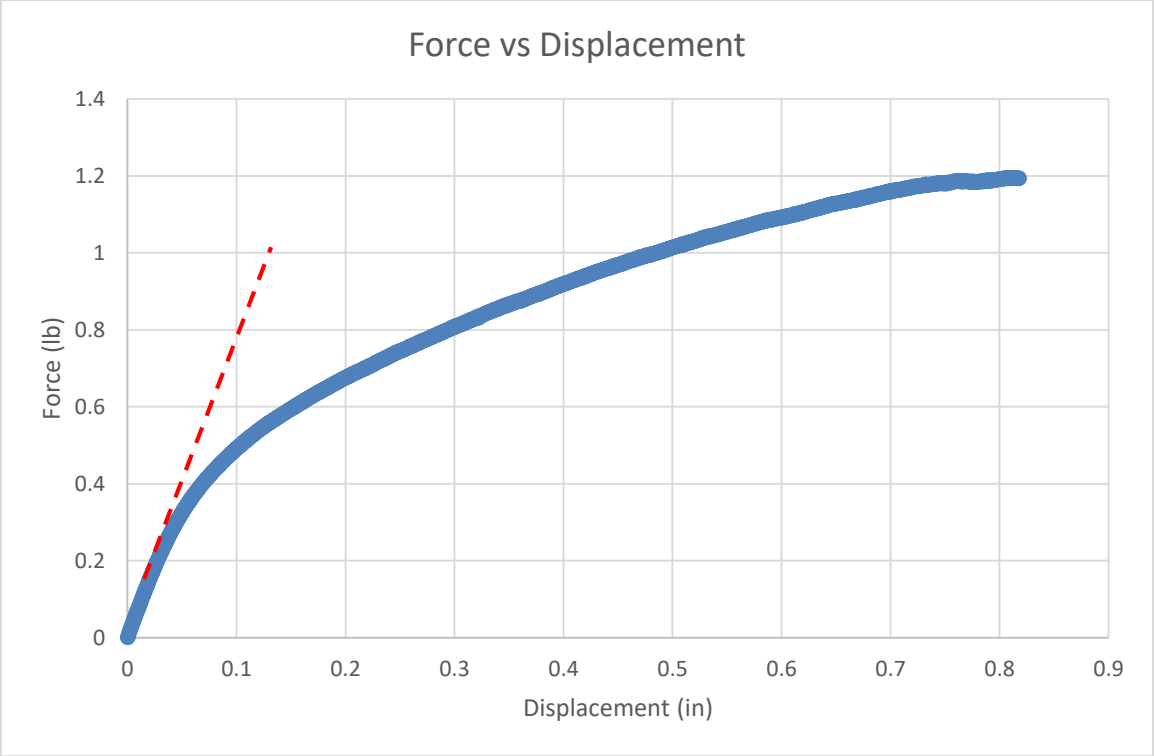

Figure 3.10: Force vs. displacement graph of a nonwoven web sample

RESONANCE DYNAMIC TESTING:

TAPPI [1] proposed a method to determine the bending stiffness of paper and paperboard by the resonance length method. The experiment can be used for materials of low grammage. The SMS nonwoven web has grammage of 15.7 g/m^2. In this experiment, the sample is clamped at one end as shown in Figure 3.11 and vibrated. The resonance length is the length of the free end of the test piece at resonance.

The bending stiffness S^b of the material is determined by the expression: [1]

$$S^b = \frac{4\pi^2}{k^4} l^4 w' f^2 \times 10^{-12} \quad (3.2)$$

where, l is the resonance length of a rectangular sample in mm, w' is the grammage in g/m^2, f is the vibration frequency (constant value: 25 Hz) and k is the dimensionless constant which is equal to 1.875 for the fundamental frequency of oscillation [1].

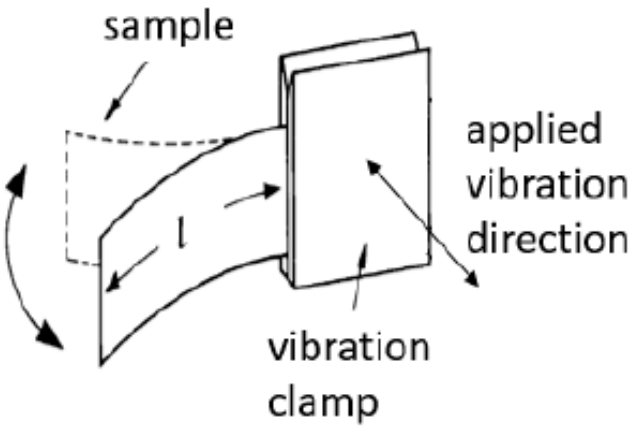

Figure 3.11: Resonance Dynamic Testing [1]

EXPERIMENTAL SETUP:

In this experiment, a signal generator shown in Figure 3.12 is used to vary the frequency and amplitude. The signal generator is connected to the vibrating shaker. The web sample is attached to the clamps using a double-sided tape and the clamp is mounted on the vibrating shaker shown in Figure 3.14. The shaker will start to vibrate when it is connected to the shaker and by changing the frequency on the signal generator, the shaker vibrates at a varied frequency. The clamps shown in the Figure 3.13 are made of aluminum and is mounted on the shaker by means of a screw.

Figure 3.12: Signal generator

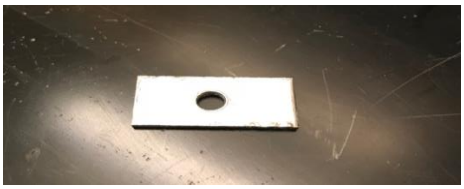

Figure 3.13: Rectangular clamp

Figure 3.14: Shaker

A test sample is clamped at one end and the length of the free end of the sample is denoted as l. The vibration of the sample is similar to the free vibration of a cantilever beam, for which the previous studies have given the relationship between resonance frequency f and the bending stiffness as [10],

$$\frac{Et^3}{12(1-\nu^2)} = \frac{4\pi^2 f^2}{k^4}.w'.l^4 \tag{3.3}$$

Where ν is the effective Poisson's ratio which is assumed to be 0.48 in this work, because the FEA software would not take any Poisson's ratio > 0.5.

PROCEDURE:

The experiment should be conducted in the atmosphere 50% RH, 23°C. In this experiment, a nonwoven web sample of 1×0.5 in is considered. The nonwoven web sample is clamped and mounted on the shaker as shown in Figure 3.14. Ensure that the sample is fixed perpendicular to

the clamps. As mentioned in [1], the clamp is vibrated at a frequency of 25 Hz with an amplitude not exceeding 0.2 mm (0.008 in.). Perform the experiment by varying the length of the sample till the sample goes into resonance, i.e. when the maximum amplitude of vibration is reached as shown in Figure 3.15 (a). The modes of vibration shown in Figure 3.15 (b) is higher mode vibration. The length of the specimen is reduced by 0.1 in every time using the scissor. Make sure that the specimen is cut precisely. Once the sample reaches the maximum amplitude, the sample is removed from the clamp and the length of the free end is measured accurately. The procedure is repeated for samples of relevant thickness and the average value of bending stiffness is calculated for different thickness from equation (3.2).

The combined parameter $E.t^3$ is obtained for different densities from equation (3.3). By using this equation and the equation from the tensile test, the moduli E and thickness t can be determined for different thickness.

A correlation can be established between local thickness and effective moduli / thickness in local region of the web. The material properties obtained from these experiments can be implemented in the dynamic simulation.

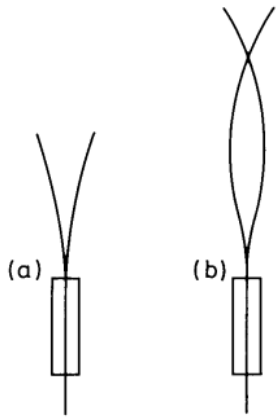

Figure 3.15: Modes of specimen vibration (a) correct (b) incorrect [1]

Preliminary tests are conducted to check if the gravity of the web sample is affecting the bending stiffness of the samples. The web is clamped between the rectangular clamps using a double-sided tape. The nonwoven web sample is aligned in three different directions as shown in Figure 3.16, to find out the resonance frequency for two samples of a fixed size 1×0.5 in^2. For each test at one of the three positions, the frequency is varied until the maximum amplitude (resonance) is achieved to see if the test is resonance vibration is dependent on the direction of gravity force. The resonance frequency values are recorded in Table 3.1. From the tests, it is found that the alignments of the web do not affect the resonance frequency and therefore gravity force will not affect the measured resonance length or eventually the bending stiffness.

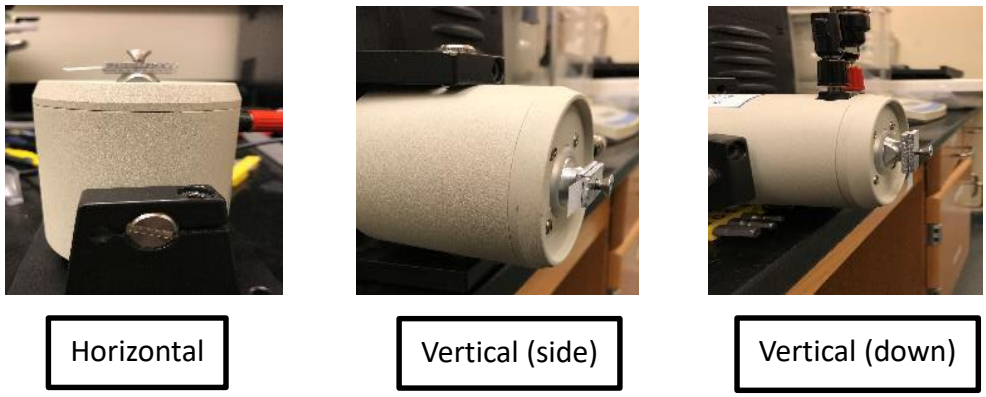

Figure 3.16: Web aligned in 3 directions

Table 3.1: Resonance frequency at different positions

	Sample 1 *f* (Hz)	**Sample 2** *f* (Hz)
Horizontal	19.5	32
Vertical (side)	20.5	32.5
Vertical (down)	21	32

EXPERIMENTAL METHOD TO DETERMINE THE CRITICAL TROUGHING LOADS:

The nonwoven web starts to buckle and form troughs, when a uniaxial tensile load is applied. The web starts to form troughs at small load. This experiment is carried out to determine at what load the troughs starts to form. The nonwoven web is clamped at one end on a horizontal flat surface. A uniaxial tensile load is applied manually by means of a digital force gauge (Shimpo FGV-20) to record the force value at which the troughs formed are visible. The force at which the troughs are formed is compared with the finite element results later in the Chapter V.

EXPERIMENTAL SETUP:

A nonwoven web sample of 23×7.5 in is used in this experiment. The nonwoven web is clamped between the rectangular clamps as shown in Figure 3.17. It is then clamped to the edge of the table by using a C-shaped clamp as shown in the Figure 3.17. One end of the web is attached to the flat rectangular plate by using tape firmly. This plate is connected to the force gauge using a thread as shown in Figure 3.18. In order to make the web flat, on the other end of the web a rectangular plate is fixed in order that the web is parallel to the horizontal surface on the table.

Figure 3.17: Experimental setup of trough test

Figure 3.18: Sideview of nonwoven web stretched in MD

PROCEDURE:

After clamping the web placed between the rectangular webs to the edge of the table, the web is stretched in the horizontal direction using the force gauge. The displacement is applied in a direction parallel to the web in MD and orthogonal to the web in CMD. The web is stretched until the troughs are formed as shown in Figure 3.19 and the displacement is marked and force at that point is noted. This experiment is conducted for 5 different samples. The displacement and force are recorded for each sample and the average value is calculated.

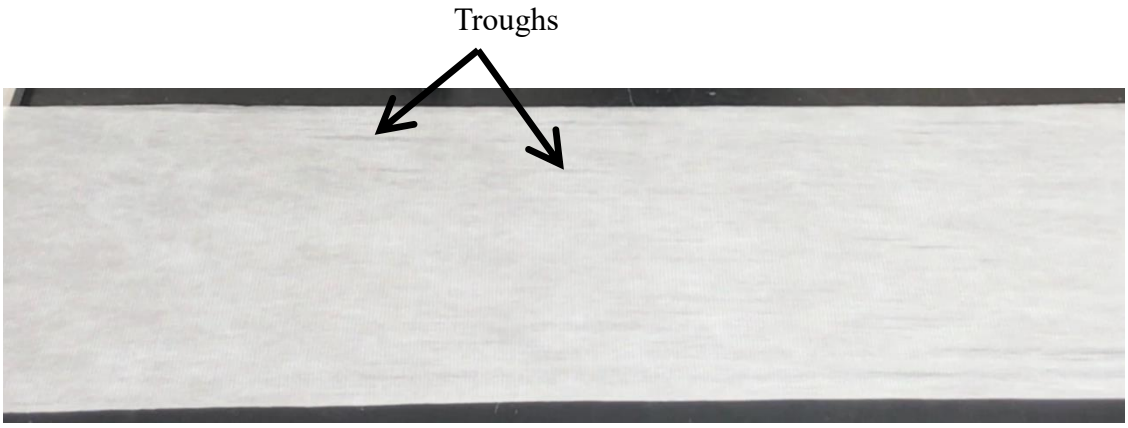

Figure 3.19: Trough formed when load is applied

EXPERIMENTAL METHOD TO ANALYZE THE TROUGH PROFILE:

The trough profile of a nonwoven is analyzed to compare with the simulation results. Nukala [2] performed the trough profile experiment for isotropic and orthotropic troughs. The same experiment is performed for SMS nonwoven web.

EXPERIMENTAL SETUP:

The experiment is performed on Instron Universal Testing Machine shown in Figure 3.20. It is located in the Web Handling Research Center, Oklahoma State University. The experiment requires a data acquisition system, load cell, motion transducers and user interface to record the trough profile. In this experiment, a uniaxial tensile load is applied uniformly in MD to measure the out of plane displacement at an applied load. The web is clamped at both edges and the clamps are fixed to the Instron tensile machine as shown in Figure 3.20 to apply tension. The web is placed between the two rectangular clamps on each side and fixed to the clamps by using strong adhesive. The web should be orthogonal to the clamps while placing it between the clamps. After fixing the web to the clamps, it is mounted on the Instron machine. A load cell is attached between the upper clamp and the mount to record the low-level loads accurately. A Keyence laser LK-031 was used to scan the trough profile, when the web is subjected to tension. The laser beam of light emitting from the laser hits the nonwoven web and reflects back to the sensor. The laser sensor is mounted as shown in Figure 3.20. The laser sensor is moved horizontally on the linear bearing to record the out-of-displacement data along the width of the web. A Yo-Yo pot 1850-0500 (motion transducer) is used to measure the horizontal position of the laser sensor. The vertical position of the laser sensor is measured by using motion transducer P-50A. The slides are fixed to the Instron as shown in Figure 3.20.

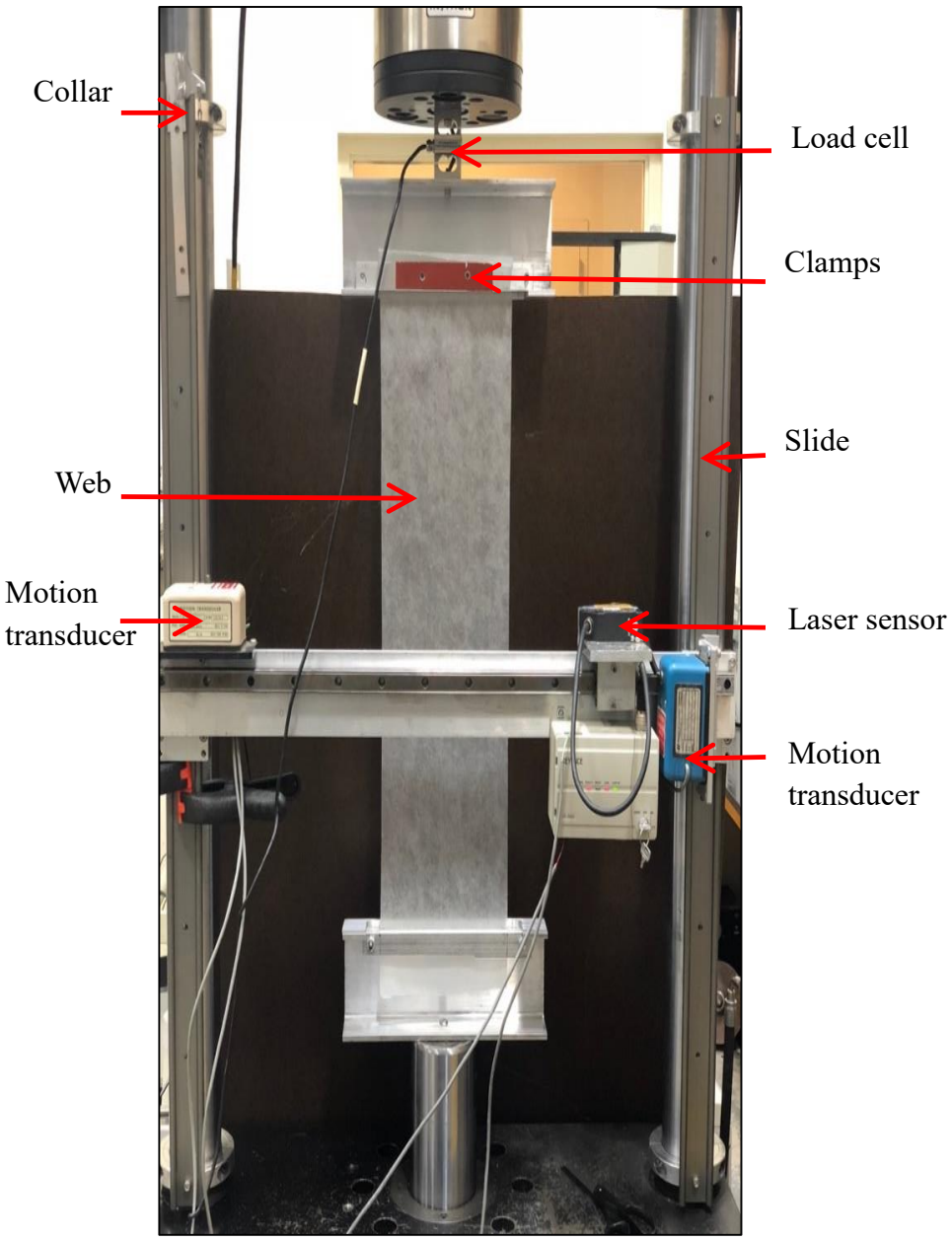

Figure 3.20: Experimental setup

Using the Lab-view program shown in Figure 3.21 and DAQ with NI SCB-68 A/O board, the out-of-plane displacement, horizontal position of the laser sensor measured from Yo-Yo pot 1850-0500, vertical position of the laser sensor measured from motion transducer P-50A is recorded.

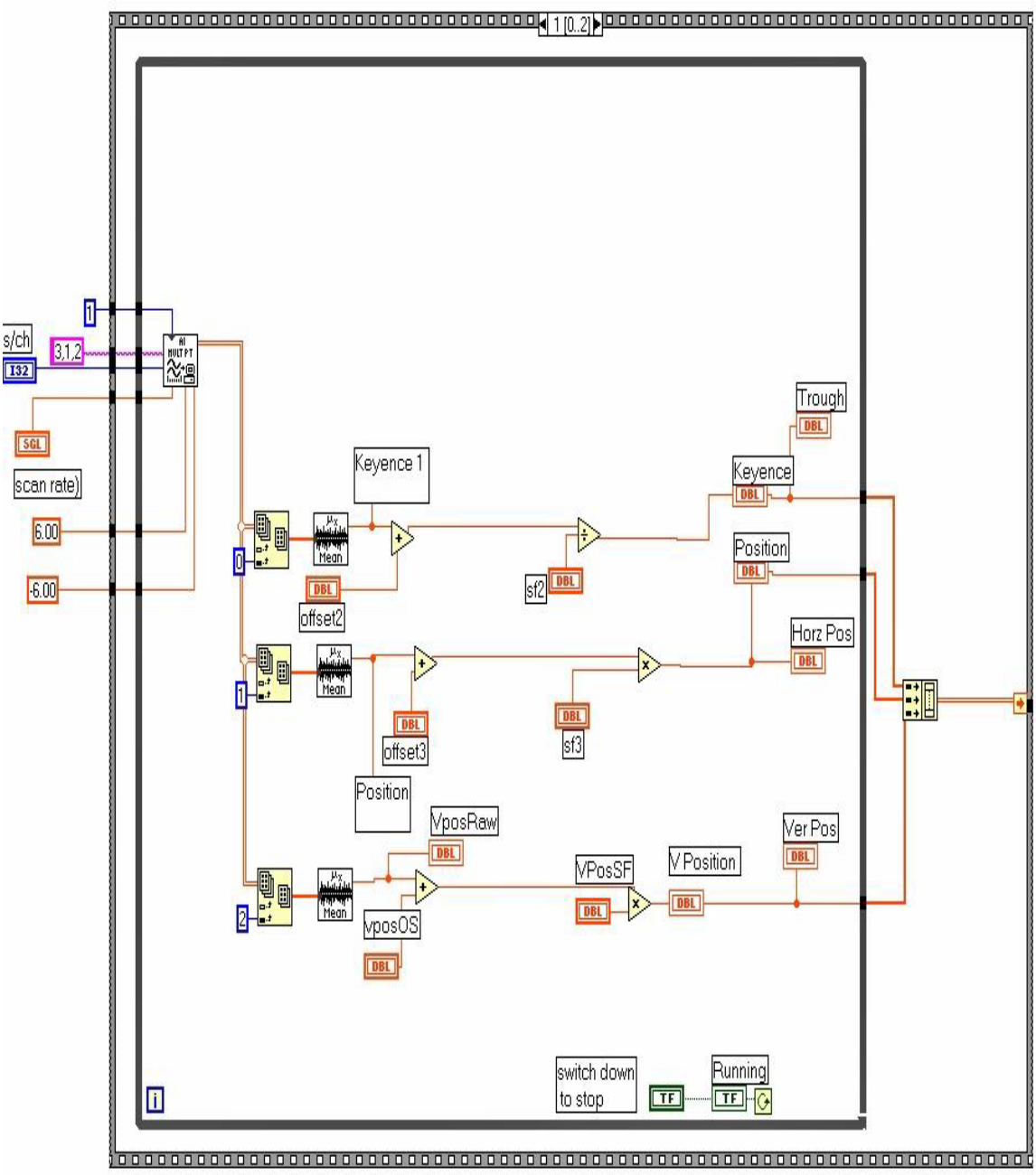

Figure 3.21: LabVIEW program for trough profile

RECTANGULAR CLAMPS:

Figure 3.22: Splice table

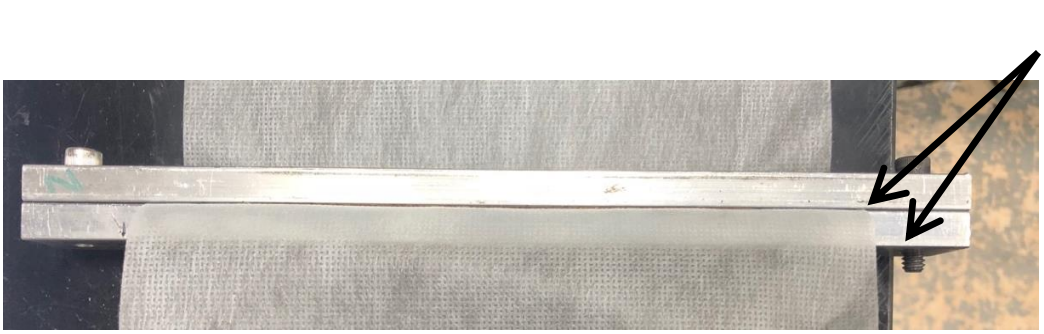

(a)

(b)

Figure 3.23: (a) (b) Rectangular clamps

A splice table was used as shown in Figure 3.22 to place the web between the aluminum clamps in order that the web is orthogonal to the clamps. The aluminum clamps shown in Figure 3.23(b) are used to clamp the web. A double-sided tape is used to fix the web between the clamps in order to avoid slippage and the rectangular clamps are tightened by the screws on both sides as shown in Figure 3.23(a).

PROCEDURE:

The nonwoven web sample of length 23 in and width 7.5 in was used in this experiment. The samples used in this experiment are first scanned using MeSys to record the thickness data. The sample is clamped to the rectangular samples and is mounted on the Instron machine. The vertical position of the laser sensor should be at the midpoint of the web along the MD. Uniform loads ranging from 1 to5 lbf are applied to create the trough profiles. For each load, the out of plane displacement data are recorded along the width of the web by moving the laser sensor along the horizontal position. The recorded data is plotted to analyze the trough profile at each load. The test is carried out for three different samples. These trough profile results are compared with the ABAQUS results.

CHAPTER IV

FINITE ELEMENT SIMULATION

4.1 FINITE ELEMENT SIMULATION CONSIDERING THE SMS WEB AS ISOTROPIC

FINITE ELEMENT ANALYSIS USING ABAQUS:

An ABAQUS software was used to model the nonwoven webs and to predict the trough formation. The 2D planar stress analysis is performed to analyze the compressive stress in CMD. The buckling analysis is performed to analyze the trough profile of a nonwoven web and obtain the buckle modes. And finally, a post-buckling analysis is performed to obtain the trough profiles under given loads.

PLANE STRESS ANALYSIS:

For 2D plane stress analysis, a solid section was created. Three different models of different grid sizes are created for the plane stress analysis. Those models are web of size 21×7 in divided into grid size of 3×0.5 in and 23×7 in divided into grid sizes of 1×0.5 in and 1×0.25 in. Mesh is generated such that each grid is divided into 10 elements in x-direction and 5 elements in y-directions. The parameters used for stress analysis is shown in Table 4.1 below.

From tensile test and the bending test,

$$EA = \frac{FL}{U} \tag{4.1}$$

$$EI = \frac{Et^3}{12(1-\nu^2)} = \frac{4\pi^2 f^2}{k^4}.w'.l^4 \tag{4.2}$$

EI is considered as constant for any thickness value. EA for different thickness readings is obtained from equation (5.1). Equating the equations will result in the effective modulus and thickness at different thickness readings. The thickness and modulus is obtained by the following equations using equation (4.1) and (4.2):

$$t_{ij} = \sqrt{\frac{12EI_{ij}(1-\nu^2) \times w}{EA}} \tag{4.3}$$

$$E_{ij} = \frac{EA}{w \times t_{ij}} \tag{4.4}$$

where, E_{ij} and t_{ij} are the modulus and thickness and and w=0.5 in is the test specimen width.

Table 4.1: Parameters used for stress analysis

Model	Length (in)	Width (in)	Modulus (psi)	Thickness (in)	Poisson's ratio
Solid section	23	7	Obtained from equation (4.4)	Obtained from equation (4.3)	0.48

Thickness distribution data is collected for a sample. The sample is divided into respective grid size and the average thickness of each grid is calculated which provides a thickness distribution map. The material properties are assigned to the model and the model is created using python code. For each thickness reading in the thickness map, respective moduli and thickness values are implemented as shown in Figure 4.1 using the equations (5.1) derived from the experiments in the python code. An inp file is generated from the python code and imported into ABAQUS to generate the model.

The left end of the web is fixed in both x and y directions and the right end of the web is fixed in y direction. Two ends of the web in MD are free boundaries. The stress analysis is performed to analyze the CMD stress which results in buckling.

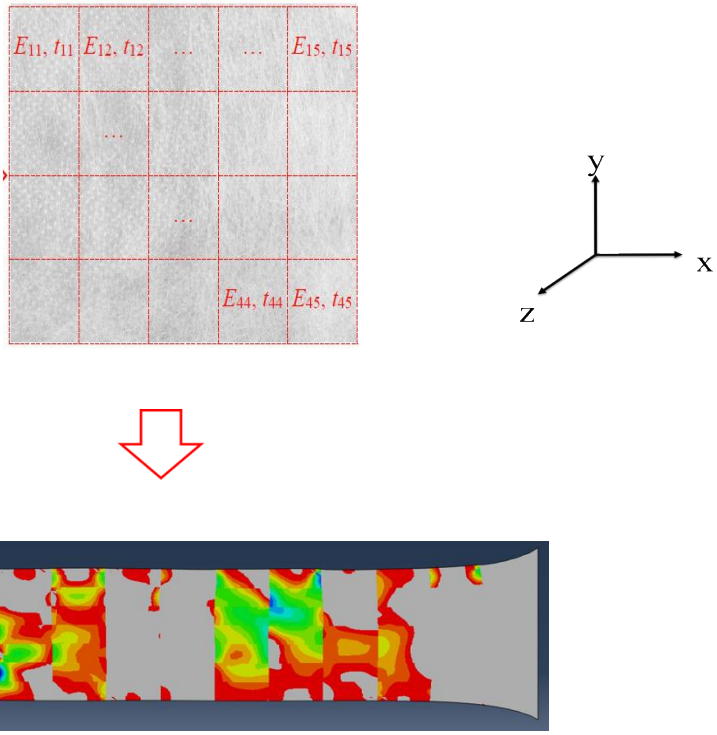

Figure 4.1: Implementation of moduli and thickness in FEA model for plane stress analysis

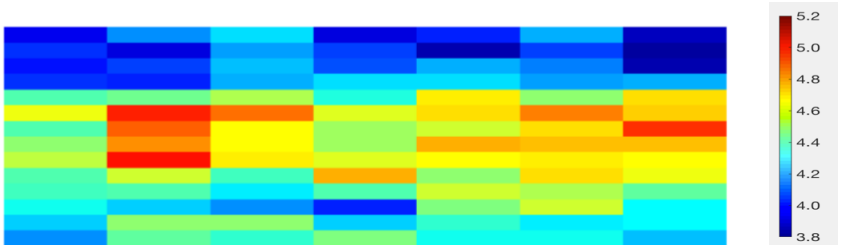

(a)

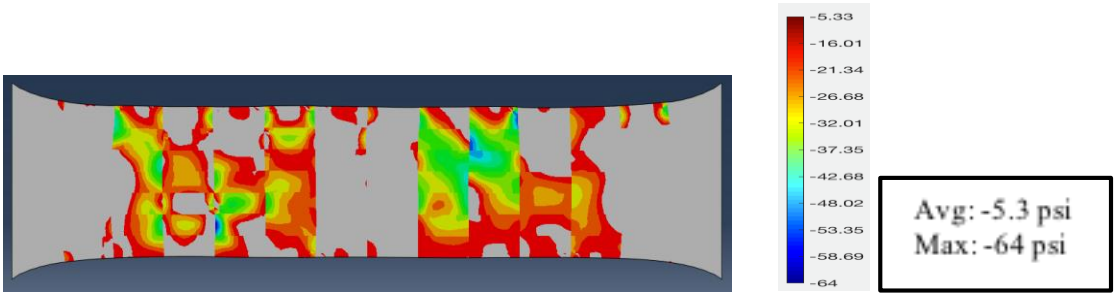

(b)

Figure 4.2: (a) Thickness map of 3x0.5 grid size (b) CMD stress in ABAQUS

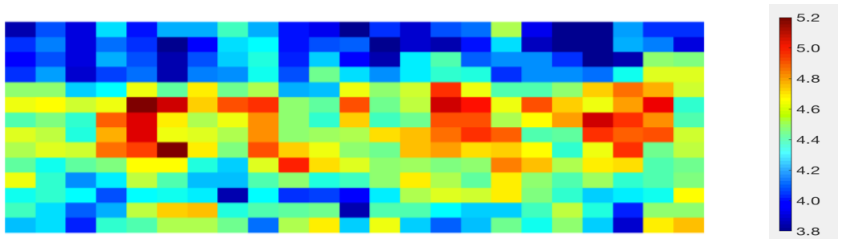

(a)

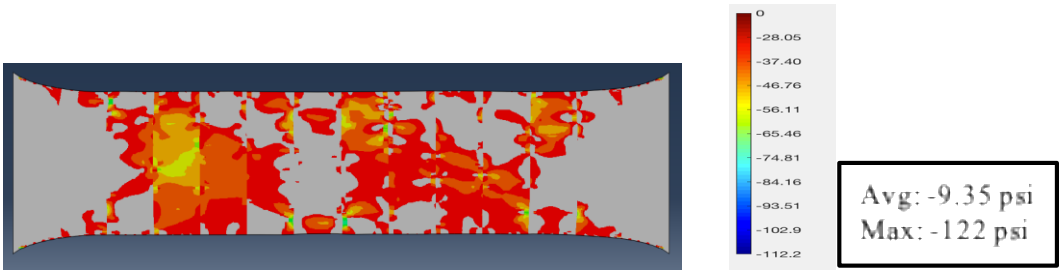

(b)

Figure 4.3: (a) Thickness map of 1x0.5 grid size (b) CMD stress in ABAQUS

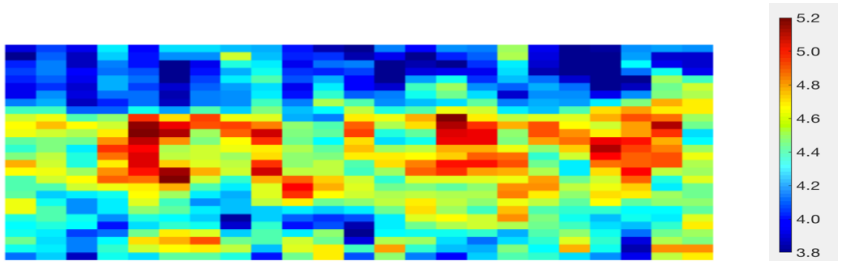

(a)

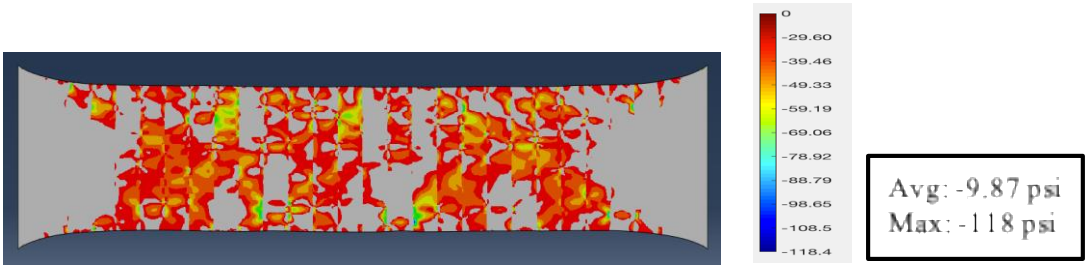

(b)

Figure 4.4: (a) Thickness map of 1x0.25 grid size (b) CMD stress in ABAQUS

The CMD compressive stress for different grid sizes of nonwoven web is shown in Figures 4.2-4.4. The more negative value the more compressive stress. The average value of CMD

compressive stress is calculated for each grid size. The compressive stress value displayed in Figures 4.2(b)-4.4(b) is the stress value for 1 in stretch along the MD. The stress is considered linear to the displacement, i.e., for example the maximum CMD compressive stress of 1×0.25 in grid size is 118 psi for a 1 in linear displacement. Therefore, for 10 in linear displacement, the CMD compressive stress is 1180psi. The total force used to stretch the web is calculated by summing up the reaction forces at the right end of the model where the displacement is applied.

SKEWED DEFORMATION AT SPOT OF MAX CMD COMPRESSION:

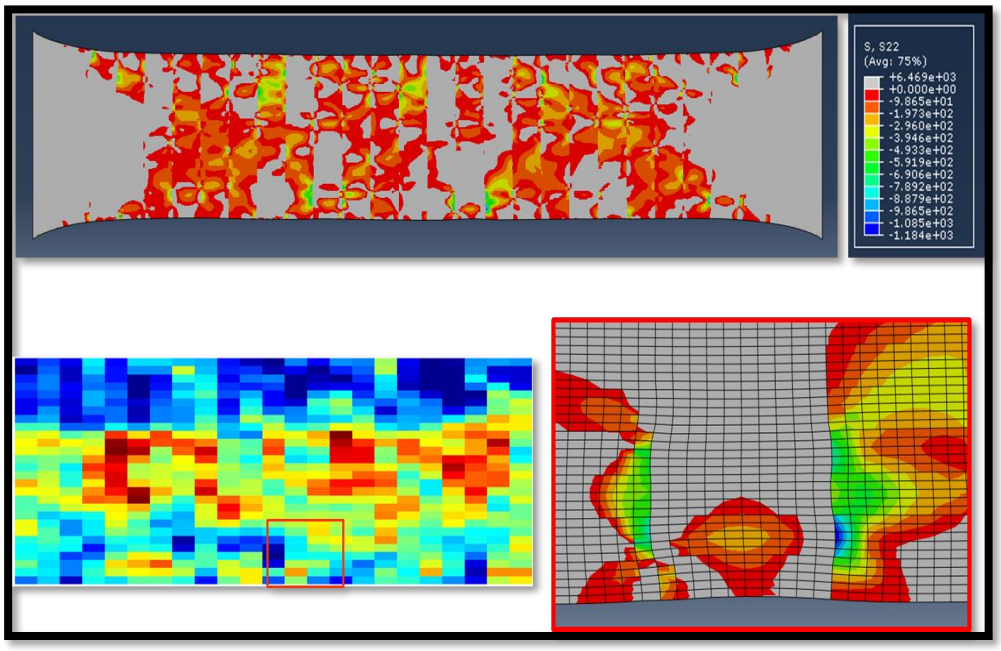

Figure 4.5: Deformation at spot of max CMD compression

The deformation at a spot of CMD compression is shown in Figure 4.5. It can be seen that the thickness distribution area is not high where the CMD compression is maximum.

BUCKLING ANALYSIS:

The buckling analysis is performed to analyze the troughs of different samples at an applied load. For buckling analysis, a 3D model with shell elements is created. The same material thickness and modulus as in the 2D stress analysis are used here.

The thickness distribution map of samples used in the experiment to analyze trough profile is used in the buckling analysis. The model was created in the same way as it is created for the plane stress analysis. The left end of the web is fixed in three directions and the right end is fixed in y and z directions. From buckling analysis, the load at which the web starts to show initial troughs can be determined. The buckling of a sample nonwoven web is shown in Figure 4.6. FEA predicted that a very small load ~ 0.1 lbf/in results in initial troughs.

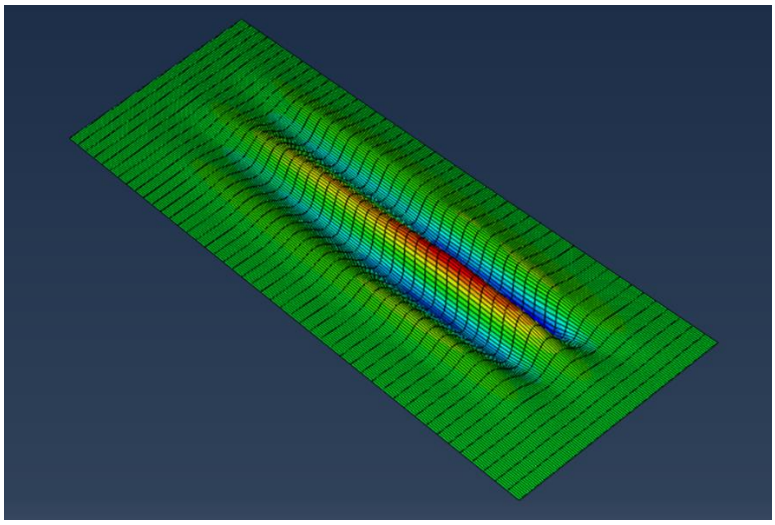

Figure 4.6: Buckling analysis of a nonwoven web

PREDICTED AND MEASURED LOAD FOR ONSET OF TROUGH:

According to Good and Biesel's model [3], [4] on trough formation, the critical CMD stress for forming trough is:

$$\sigma_{y,cr} \approx -2\sqrt{\sigma_x \sigma_e} \tag{4.5}$$

where,

$$\sigma_e = \frac{\pi^2 D}{a^2 t} \tag{4.6}$$

where,

$$D = \frac{Et^3}{12(1-\nu^2)} \tag{4.7}$$

Here, a is considered as the length of the grid size in order to predict the localized troughs. σ_x is the average MD stress. ν is the Poisson's ratio which is assumed to be 0.48 and t is the thickness of the material.

If the stress in CMD is more compressive than the stress in the equation, the web begins to buckle which results in troughs. The critical load at which the troughs formed in different cases is shown in Table 4.2 below.

Table 4.2: Comparison of estimated stretch and critical load which results in troughs for different samples

	Critical load based on average CMD stress in pre-buckle FEA and Eqn. 4.5		Critical load based on maximum CMD stress with pre-buckle FEA and Eqn. 4.5		Critical loads from FEA buckling analysis	
	Stretch (in)	Load (lbf/in)	Stretch (in)	Load (lbf/in)	Stretch (in)	Load (lbf/in)
web-1	5.38	12.2	0.037	0.078	0.024	0.05
web-2	6.32	14.3	0.044	0.100	0.033	0.075
web-3	9.11	20.6	0.063	0.142	0.032	0.072

From the FEA simulation of different samples, in the case of average CMD stress, the troughs started to initiate at a larger load. It was observed that troughs are predicted almost instantaneously at localized location when the web is stretched in the MD. FEA predicted that a

very small load ~0.1 lbf/in results in initial troughs, which approximately agrees with the critical loads predicted by equation (4.5) and 2D plane-stress FEA predicted maximum CMD stress. These loads will be compared to experiments in the experimental section.

POST BUCKLING ANALYSIS:

Post buckling analysis is carried out to analyze the troughs at different loads after initial buckling. The models which are used in the buckling analysis are used in the post buckling analysis, and the first 15 buckling modes are introduced as "imperfection" in the initial state. The amplitudes, locations, and wavelengths of the troughs in the nonwoven web can be obtained for given loads. From post-buckling analysis in ABAQUS, the out of plane displacement can be obtained from the output. The out of plane displacement at the mid-span of the web in MD across the width of the web in CMD is also produced as the output and compared to corresponding experimental measurements. The wavelength and amplitude is calculated from each out of displacement graph and the FEA results are compared with the experimental results, which are detailed in the next Chapter.

4.2 FINITE ELEMENT SIMULATION CONSIDERING THE SMS WEB AS ORTHOTROPIC

4.2.1 UNIFORM ORTHOTROPIC WEB

FINITE ELEMENT ANALYSIS:

The case of a uniform orthotropic web is studied by using the mesh-generating python codes. In this analysis, the thickness and moduli in MD and CMD do not vary at different locations of the web. Buckling analysis and post buckling analysis is performed to determine the trough profiles, and compared to theory and experiments in the Results Chapter.

BUCKLING ANALYSIS:

The buckling analysis with a fine mesh (element size of 0.03x0.05 in^2) is performed to obtain the trough profiles. The parameters used for buckling analysis are shown in Table 4.3 [4]. The buckling analysis provides only two Eigen modes which are shown in Figure 4.7.

Table 4.3: Parameters used for buckling analysis

Model	Length (in)	Width (in)	E_x (psi)	E_y (psi)	Thickness (in)	Poisson's ratio ν_{xy}	Poisson's Ratio ν_{yx}
Shell section	23	7	7991.57	1199	0.0047	0.3	0.04

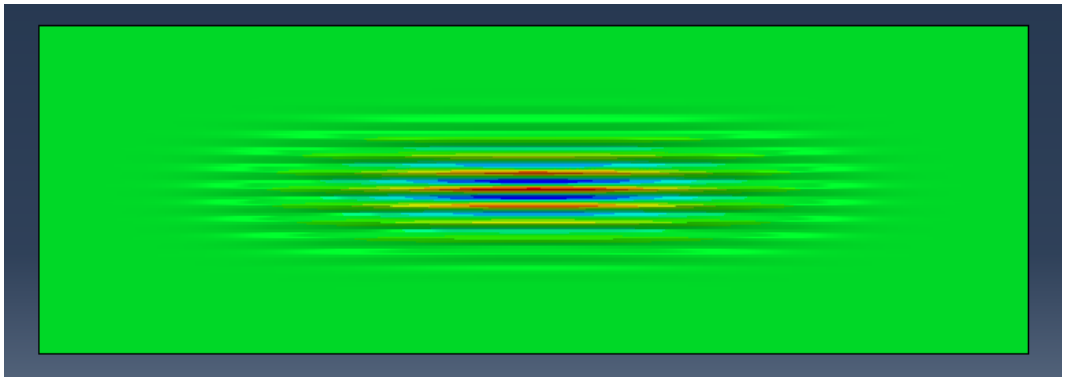

(a)

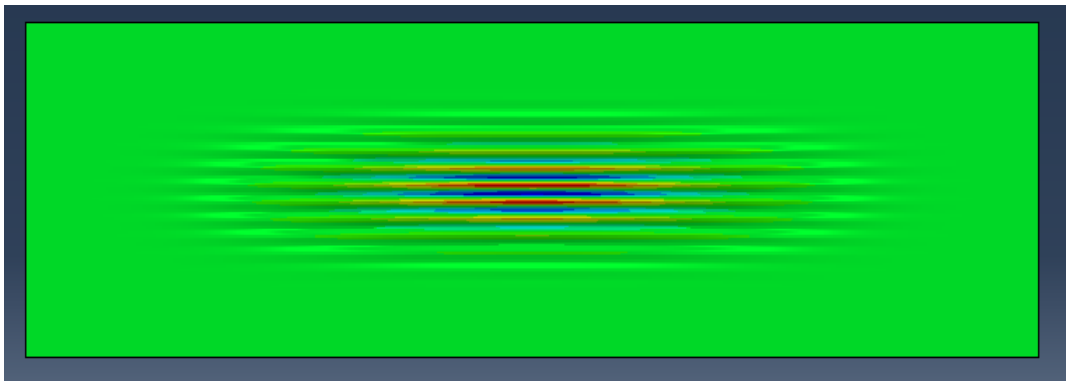

(b)

Figure 4.7: Buckling analysis of uniform nonwoven web at different modes

POST-BUCKLING ANALYSIS:

Post-buckling analysis is carried out to analyze the troughs at different loads by introducing small *imperfection (1 mil) of the buckling modes into the initial shape of web. The same material properties specified in the Table 4.3 are used in the post-buckling analysis. The post-buckling analysis of a nonwoven web at a load of 5 lbf is shown in Figure 4.8. The buckling profiles are compared to the experiments in the next Chapter.

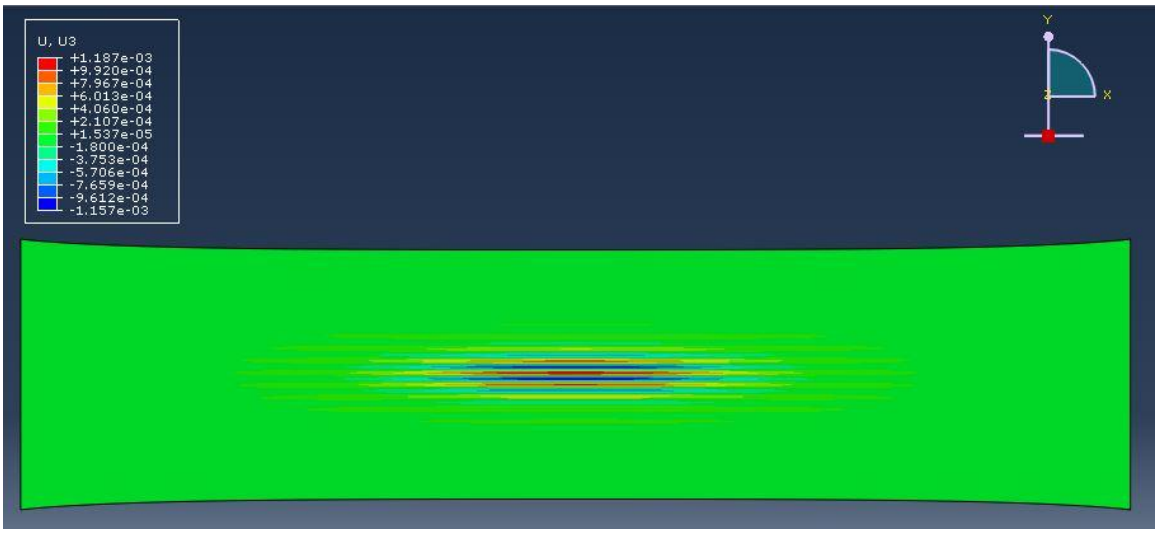

Figure 4.8: Post-buckling at a load of 5 lbf

4.2.2 NON-UNIFORM ORTHOTROPIC WEB

FINITE ELEMENT ANALYSIS:

The nonwoven web is considered as the orthotropic material whose properties changes when measured in different directions. Because the bending stiffness measurements do not yield satisfactory results, here the scanned value of thicknesses are adopted directly as the thickness *t* instead. In finite element analysis, the modulus in MD (E_x) and CMD (E_y) and thickness (t) is considered. It is considered as non-uniform orthotropic material. By using the equation (3.1), the

EA value for different thickness readings is calculated. From the equation (5.1) and (3.1), the modulus (E_x) for any thickness value can be obtained by:

$$E_x = \frac{\text{EA}}{w * t} \tag{4.8}$$

where t is the measured thickness of the grid obtained by the MeSys scanner and w=0.5 in is the width the testing specimen.

In Good and Beisel [4], the E_x and E_y of polypropylene nonwoven is mentioned in the paper. $E_x = 55.1$ MPa and $E_y = 8.27$ MPa. The E_y value is almost $1/6^{th}$ of the E_x value. In our research, only the modulus (E_x) is obtained from experimental tests. Assuming the overall ratio between E_y and E_x applies to the SMS web in this study, E_y is calculated from E_x by considering the E_y as shown in equation (4.9):

$$E_y = \frac{8.27}{55.1} E_x \tag{4.9}$$

ν_{yx} can be calculated from Maxwell reciprocal theorem [4] which provides a relation between the modulus and Poisson's ratio:

$$\frac{\nu_{xy}}{E_x} = \frac{\nu_{yx}}{E_y} \tag{4.10}$$

PLANE STRESS ANALYSIS:

For 2D plane stress analysis, similar to the isotropic web, a solid section was created. Three different models of different grid sizes are created for the plane stress analysis. Those models are web of size 21×7 in divided into grid size of 3×0.5 in and 23×7 in divided into grid sizes of 1×0.5 in and 1×0.25 in. Mesh is generated such that each grid is divided into 10 elements in x-direction and 5 elements in y-directions. The parameters used for stress analysis is shown in Table 4.4.

Table 4.4: Parameters used for stress analysis

Model	Length (in)	Width (in)	E_x (psi)	E_y (psi)	Thickness (in)	Poisson's ratio ν_{xy}	Poisson's Ratio ν_{yx}
Solid section	23	7	Obtained from equation (4.8)	Obtained from equation (4.9)	Obtained from thickness map	0.48	Obtained from equation (4.10)

The material properties are assigned to the model and the model is created using python code. For each thickness reading in the thickness map, respective modulus (E_x and E_y) and thickness values are implemented as shown in Figure 4.1. An inp file is generated from the python code and imported into ABAQUS to generate the model.

The left end of the web is fixed in two directions and the right end of the web is fixed in vertical direction. Two ends of the web in MD are free boundaries. The stress analysis is performed to analyze the CMD stress which results in buckling.

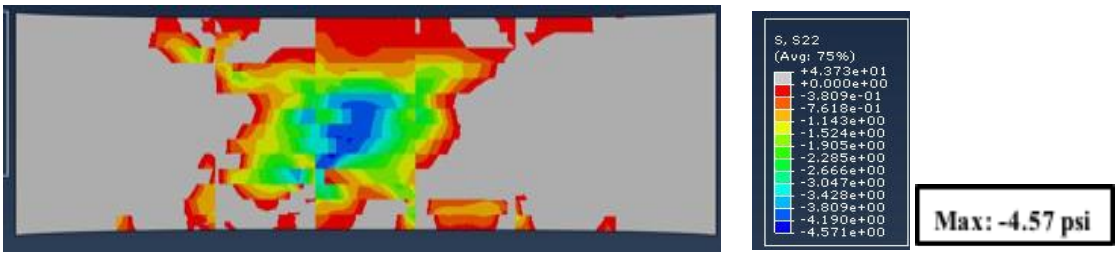

Figure 4.9: CMD stress of 3x0.5 in grid size in ABAQUS

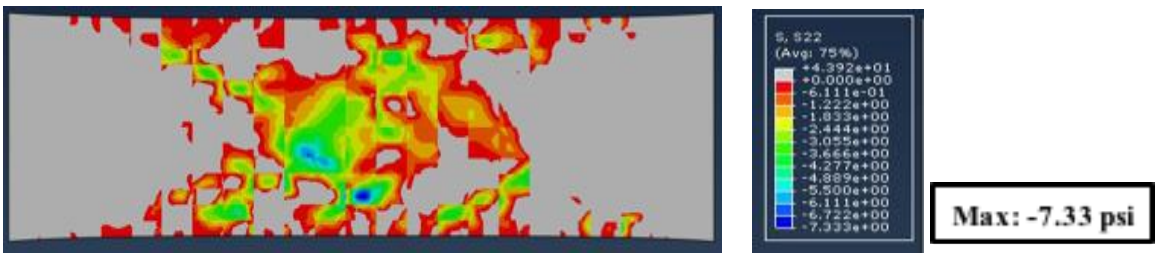

Figure 4.10: CMD stress of 1x0.5 in grid size in ABAQUS

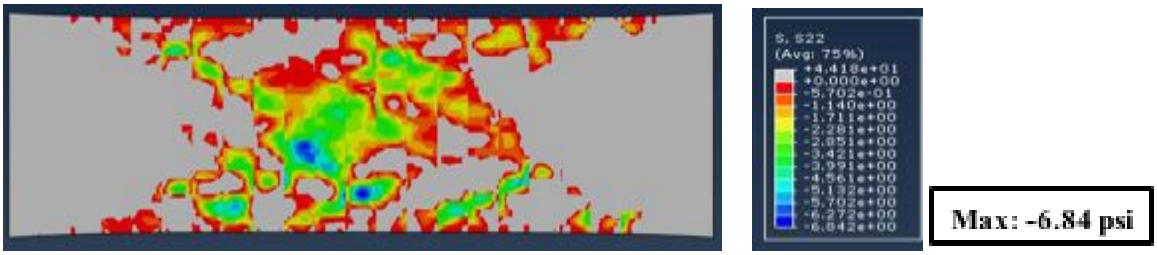

Figure 4.11: CMD stress of 1x0.25 in grid size in ABAQUS

The CMD compressive stress for different grid sizes of nonwoven web is shown in Figures 4.7-4.9. The stress value displayed in Figures 4.9-4.11 is the compressive stress value for 1 in stretch along the MD.

BUCKLING ANALLYSIS:

The buckling analysis is performed to analyze the troughs of different samples at an applied load. For buckling analysis, a 3D model with shell elements is created. The parameters used here are the same for those used for 2D stress analysis. The buckling analysis procedure is similar to the one discussed for isotropic materials. The buckling analysis is shown in Figure 4.12.

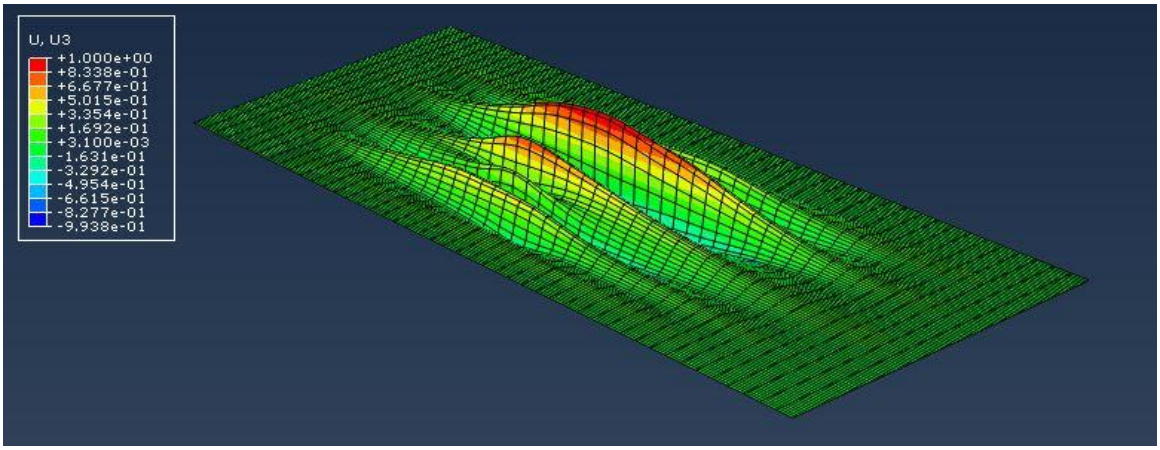

Figure 4.12: Buckling analysis of nonwoven web considering material as orthotropic

From buckling analysis, it was predicted that the initial troughs are forms at a small load of ~0.2 lbf/in.

PREDICTED AND MEASURED LOAD FOR ONSET OF TROUGH:

According to Good and Biesel's model [12] on trough formation, the critical CMD stress required to buckle the web is:

$$\sigma_{y,cr} = -\frac{\pi t}{\sqrt{3}a}\sqrt{\frac{\sigma_x E_y}{(1 - \nu_{yx}\nu_{xy})}} \tag{4.11}$$

where, σ_x is the average MD stress, a is considered as the grid length in order to predict localized troughs (which is different from the original model where a is the total length of the web), ν_{yx} and ν_{xy} are the poisson's ratio, t is the thickness of the material and ν_{xy} is considered as 0.48.

If the stress in CMD is more compressive than the stress in the equation, the web begins to buckle which results in troughs. By equating the compressive stress in CMD and equation (4.5), the displacement where the troughs are formed can be obtained. The load at the which troughs are formed can be calculated by using the displacement. The critical load at which the troughs formed in different cases is shown in Table 4.5 below.

Table 4.5: Comparison of estimated stretch and critical load which results in troughs for different samples

	Estimated critical load based on maximum CMD stress in pre-buckle FEA and Eqn. 4.11		FEA Buckling analysis (b)	
	Stretch (in)	Load (lbf/in)	Stretch (in)	Load (lbf/in)
web-1	0.946	2.134	0.109	0.245
web-2	1.313	2.962	0.082	0.184
web-3	0.234	0.527	0.089	0.2

From the Table 4.5, it was observed that troughs are predicted almost instantaneously in buckling analysis. The critical load that leads to buckling is different in both cases (a) and (b).

The inconsistency between the two approaches may be due to the following assumptions made in the analysis:

- It was assumed that, if one point in any grid buckles, the web buckles and results in troughs.
- The critical stress is highly dependent on the grid size which is artificially chosen. This assumption predicts trough formation when the CMD stress at any point in any grid reaches the buckling stress in equation (4.5), which needs to be further studied and validated by experiments.
- Poisson's ratio ν_{xy} is considered as 0.48 to approximate a nearly incompressible material. In future studies, a better method to measure the poison's ratio is required.
- E_y is calculated from E_x using equation (4.9) which is based on a spunbond nonwoven that is different from the SMS web in this study. In future studies, the E_y should be measured by a more accurate experimental method in order to get the accurate results.

POST BUCKLING ANALYSIS:

Post buckling analysis is carried out in the same method as the one with isotropic materials, except for the material properties are changed to the orthotropic properties described above. The buckling of nonwoven web at a load of 5 lbf is shown in Figure 4.13.

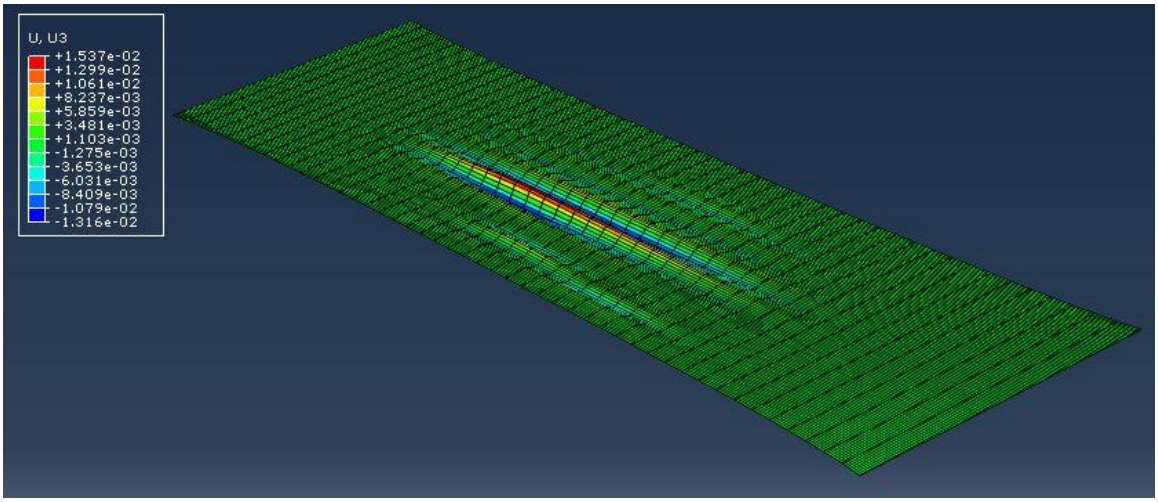

Figure 4.13: Troughs formed at a load of 5 lbf on nonwoven web

CHAPTER V

RESULTS AND COMPARISON

EXPERIMENTAL RESULTS:

TENSILE TEST:

The test is conducted for a 1×0.5 in sample. EA value is calculated for each sample of respective thickness. The average EA value is calculated for different thickness samples. The data is provided in Table 5.1.

Table 5.1: EA values of sample webs of 1x0.5 in

	Thickness (in mil)	
	4.4	5
EA (lbf)	17.956	24.086
	20.494	23.827
	19.114	18.255
	22.106	22
	24.739	25.6121
	20.183	21.724
Average EA	20.765 ± 2.392	22.584 ± 2.56

From the data, for 1×0.5 inch samples, it has been observed that the standard deviation is large and the difference between the 420 and 480 thickness samples is not statistically significant. For example, both sets of samples' EA value vary between ~18 to ~25 lbf. Therefore, it is difficult to differentiate the material properties between different thickness samples with specimen size of 1×0.5 in. 3×0.5 in samples are then considered in order to get better results. EA values for 3×0.5 in samples are noted in Table 5.2. Difference in EA values for different thickness readings can be observed from the Table 5.2.

Table 5.2: EA values of sample webs of 3×0.5 in (all samples are taken from the same web to avoid errors from normalizing. This results in different sample size)

	Thickness (mil)						
EA (lbf)	4.4	4.5	4.6	4.7	4.8	4.9	5
	25.363	24.483	27.315	26.879	25.63	27.431	33.372
	22.033	26.337	28.497	21.732	22.551	27.485	31.845
	24.332	22.989	23.877	24.408	27.774	25.968	21.276
	22.691	23.743	29.298	30.201	24.123	22.93	30.804
	19.278	23.327	25.869	29.596	27.872	29.07	27.119
	27.96	26.595	28.413	29.157	28.639	26.521	23.987
	25.785	20.413	23.871	24.674	26.028	27.485	26.205
			24.45		28.005	22.456	26.217
							26.179
							30.759
Average EA	23.92	23.983	27.211	26.663	26.088	26.168	27.776
Standard deviation	2.848	2.114	2.018	3.181	2.202	2.327	3.806

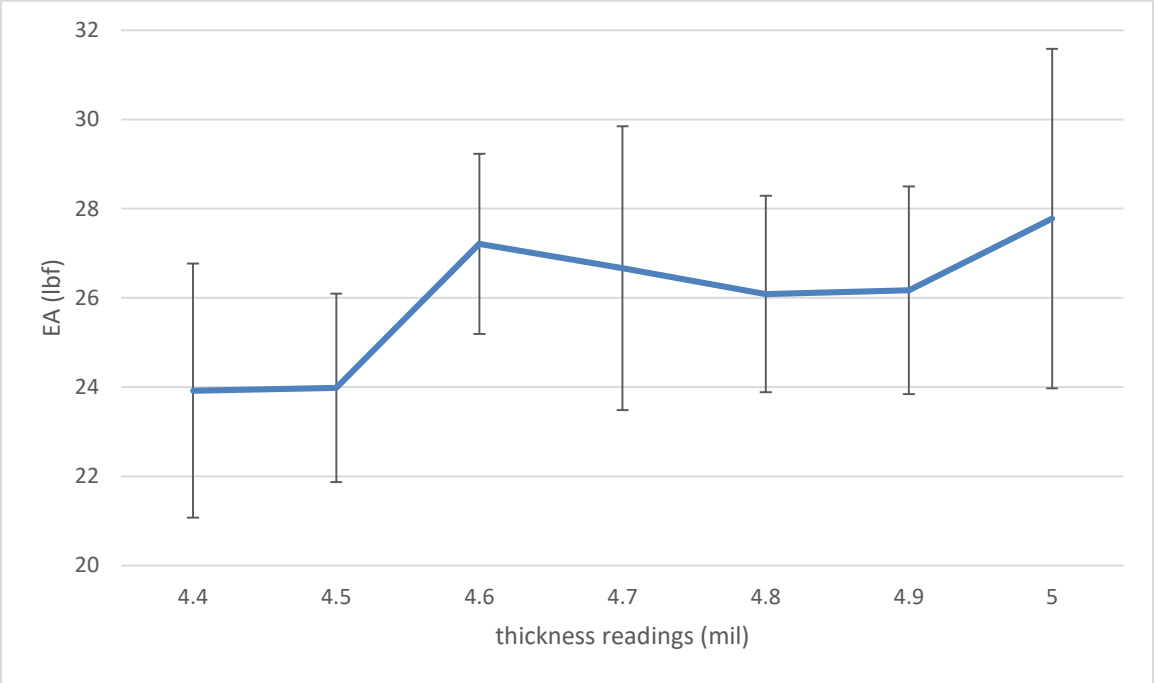

Figure 5.1: EA values for different thickness readings

Graph of average EA vs. thickness readings is shown in Figure 5.1. The curve is divided into different regions (thickness <4.4, between 4.6 and 4.8, and >4.8), and linear interpolation is used to obtain the EA values for different thickness values in inches (1 mil = 0.001 in) by the following piece-wise function:

$$\begin{aligned} EA &= 15756*t - 45.723 \text{ for } t < 0.0046 \\ EA &= -5377.8*t + 51.93 \text{ for } t < 0.0048 \\ EA &= 8081.6*t - 12.994 \text{ for } t > 0.0048 \end{aligned} \quad (5.1)$$

RESONANCE DYNAMIC TESTING:

Resonance dynamic testing is conducted for 1×0.5 in samples of different thickness readings. The bending stiffness for different thickness values is shown in Table 5.3. The average and standard deviation (S.D) is calculated for each thickness rating.

Table 5.3: Bending stiffness for sample webs of 1×0.5 in (lbf-in)

	Thickness (in mil)				
	4.4	4.5	4.7	4.9	5
Bending stiffness (lbf-in)	2.55008E-05	1.82017E-05	3.05493E-05	2.86385E-05	3.30969E-05
	2.86539E-05	2.32855E-05	1.91182E-05	2.00811E-05	2.06727E-05
	1.77841E-05	2.34334E-05	2.46605E-05	2.26457E-05	2.61093E-05
	2.27533E-05		3.03635E-05	2.01739E-05	
	1.79697E-05		3.09953E-05	2.57841E-05	
			2.44831E-05		
Average Bending Stiffness (lbf-in)	2.25323E-05	2.16402E-05	2.6695E-05	2.34647E-05	2.66263E-05
S.D.	4.73544E-06	2.97873E-06	4.75912E-06	3.71139E-06	6.22824E-06

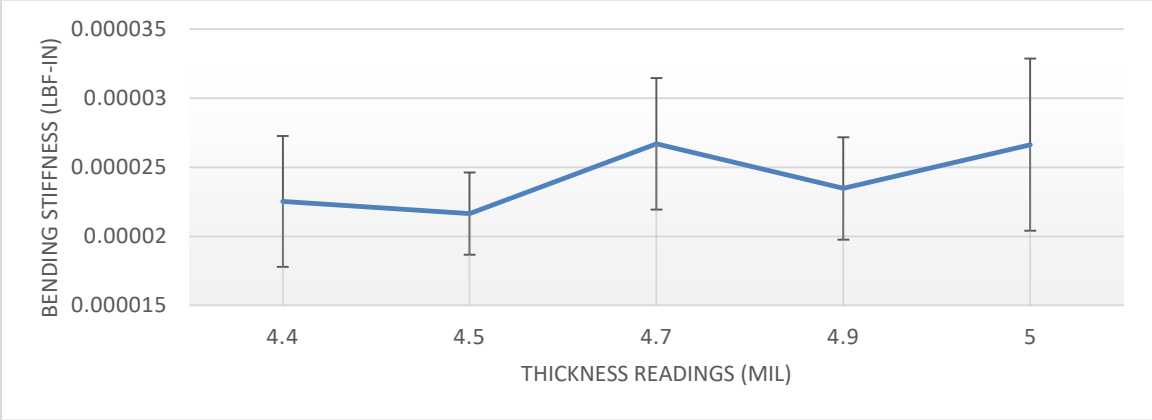

Figure 5.2: Bending stiffness (lbf-in) for different thickness readings

From Figure 5.2, it is observed that the standard variation is as large as 70% of the measured EI values. The variation of bending stiffness is not statistically significant for different

thickness values. It is hypothesized that this is mainly due to several factors. Due to the non-uniformity in the web sample, the average thickness varies as the length of the sample is reduced. This results in the change in final average thickness value. It is difficult to accurately calculate the average thickness for final sample length. Therefore, we concluded that the bending stiffness testing data cannot be used to reliably represent the property variations in the web. With the bending stiffness being such a small value, here we consider it to be constant for all the thickness readings. The average bending stiffness (2.43E-05 lbf-in) is calculated from the table and used for the entire non-woven web.

HORIZONTAL STRETCH TEST TO PREDICT TROUGHS:

A nonwoven web of length 23 in and width 7.5 in was used to measure the critical loads for the onset of trough formation. The displacement and force of 5 different samples is recorded as shown in Table 5.4. The average force for trough formation is 4.964 lbf, i.e., 0.66 lbf/in. However, this method is highly dependent on how visible the initial trough is. The critical loads at the onset of trough formation may be much smaller than these experimentally obtained value. Nevertheless, FEA buckling analysis shown in Table 4.5 using non-uniform orthotropic material properties seem to have the best prediction of these critical loads.

Table 5.4: Force and displacement of sample webs of 23×7.5 in

	Displacement (in)	Force (pli)
Samples	0.3125	0.618
	0.3125	0.624
	0.343	0.624
	0.375	0.653
	0.421	0.789
Average	0.3528	0.66

COMPARISON OF CRITICAL LOADS:

The critical load and the stretch which results in troughs obtained for isotropic and orthotropic materials are compared as shown in Table 5.5. None of these predictions are very satisfactory and future studies are proposed in the conclusion section.

Table 5.5: Comparison of estimated stretch and critical load which results in troughs for different samples

	Estimated critical load based on maximum CMD stress with pre-buckle FEA and Eqn. (4.5) and (4.11)				FEA Buckling analysis				Experimental	
	Isotropic		Orthotropic		Non-uniform Isotropic		Non-uniform Orthotropic		Average of tests on 6 SMS webs	
	Stretch (in)	Load (lbf/in)	Stretch (in)	Load (lbf/in)	Stretch (in)	Load (lbf/in)	Stretch (in)	Load (lbf/in)	Stretch (in)	Load (lbf/in)
web-1	0.037	0.078	0.946	2.134	0.024	0.05	0.109	0.245	0.3528	0.66
web-2	0.044	0.100	1.313	2.962	0.033	0.075	0.082	0.184		
web-3	0.063	0.142	0.234	0.527	0.032	0.072	0.089	0.2		

POST BUCKLING FEA -- ISOTROPIC MATERIAL:

The post buckling analysis is performed on isotropic webs to simulate the troughs at different loads. This analysis is carried out for 3 different models which are used in the experimental method to analyze the trough profile at loads of 1, 3, 5 lbf. The troughs formed on a sample nonwoven web at loads of 1, 3, 5 lbf are shown in Figures 5.3-5.5.

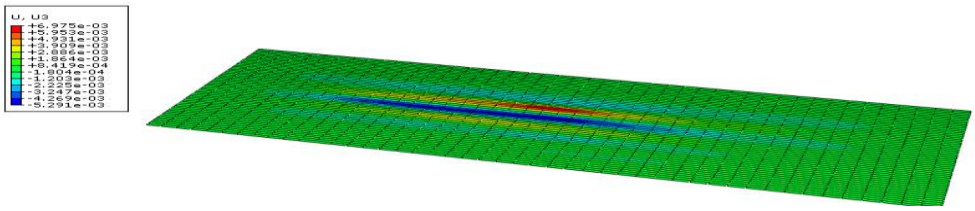

Figure 5.3: Troughs at load of 1 lbf

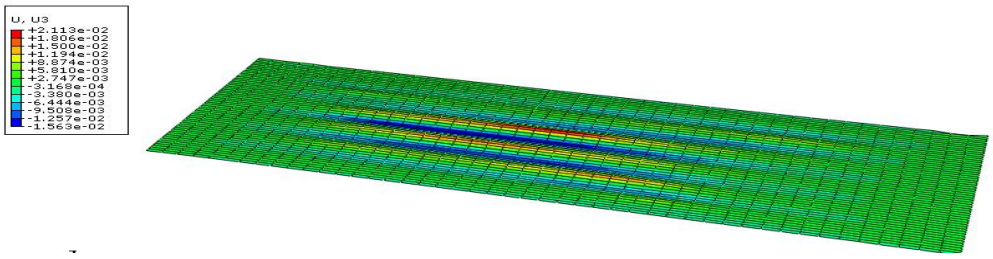

Figure 5.4: Troughs at load of 3 lbf

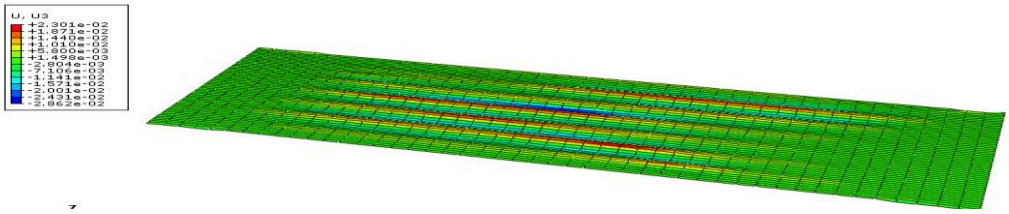

Figure 5.5: Troughs at load of 5 lbf

COMPARISON OF EXPERIMENTAL TROUGH PROFILE WITH FEA RESULTS:

A nonwoven web of 23×7.5 in was used in the experimental trough analysis and nonwoven web of 23×7 in is used in the finite element analysis. The uniform loads of 1, 3, 5 lbf are applied to the web. The trough profile was plotted for different loads. The same experiment is carried out for three samples to check the consistency. The graphs of out-of-plane displacement with respect to the width of the web at loads of 1, 3, 5 lbf from experiment are compared with the FEA results as shown in Figures 5-6 to 5-14.

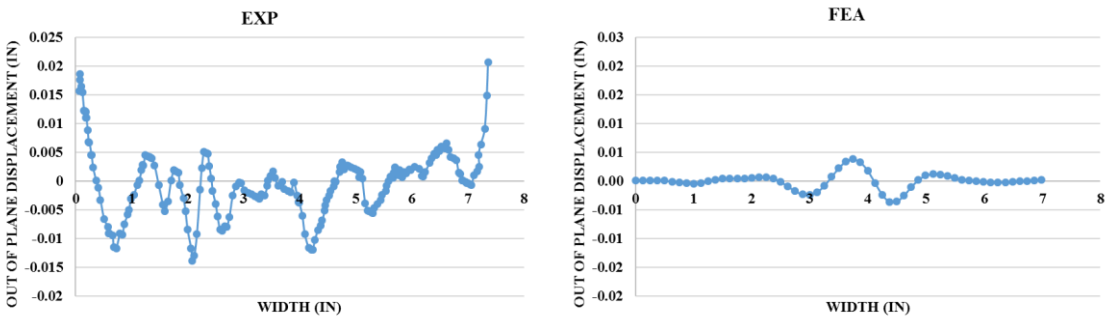

Figure 5.6: Experimental and simulation results of sample-1 at a load of 1 lbf

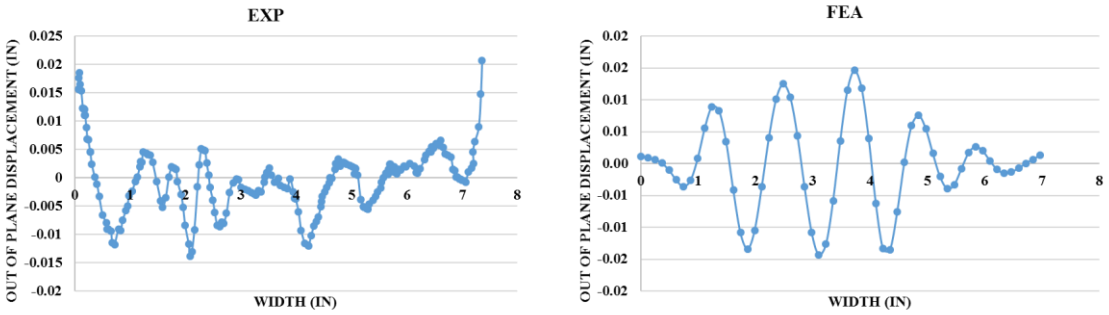

Figure 5.7: Experimental and simulation results of sample-1 at a load of 3 lbf

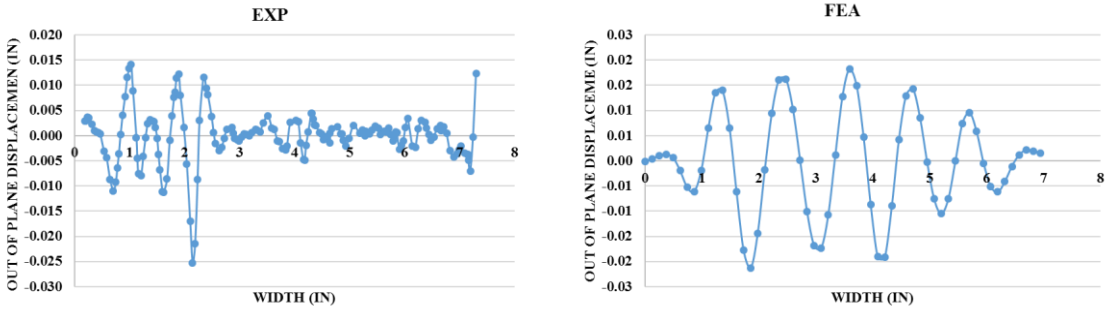

Figure 5.8: Experimental and simulation results of sample-1 at a load of 5 lbf

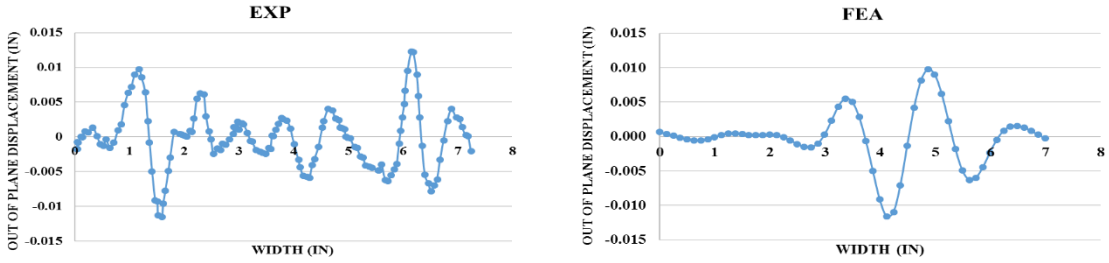

Figure 5.9: Experimental and simulation results of sample-2 at a load of 1 lbf

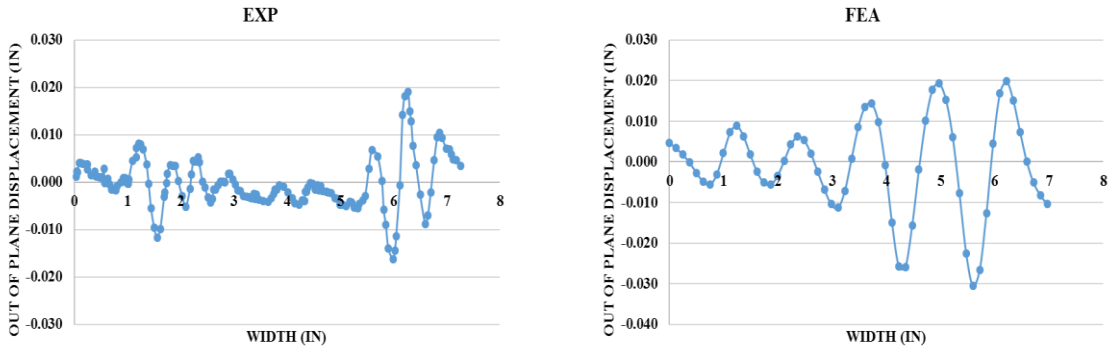

Figure 5.10: Experimental and simulation results of sample-2 at a load of 3 lbf

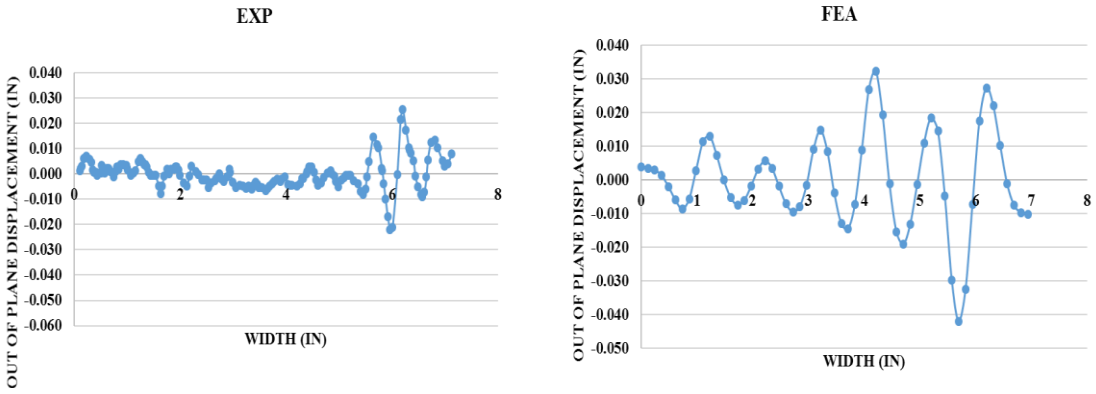

Figure 5.11: Experimental and simulation results of sample-2 at a load of 5 lbf

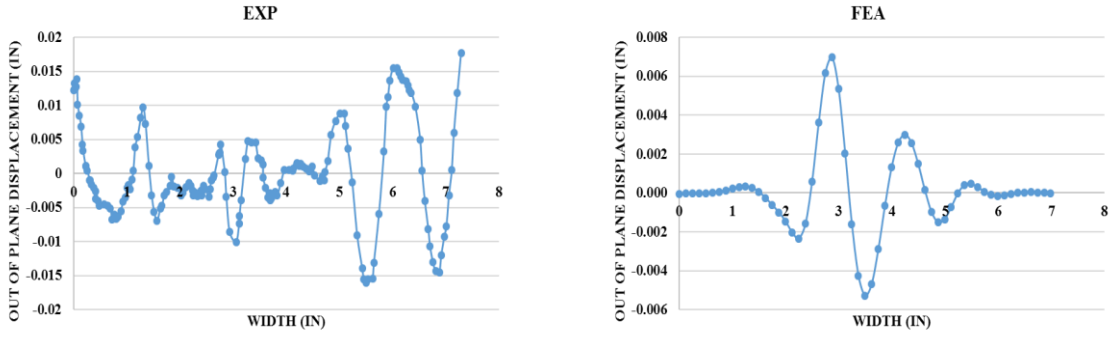

Figure 5.12: Experimental and simulation results of sample-3 at a load of 1 lbf

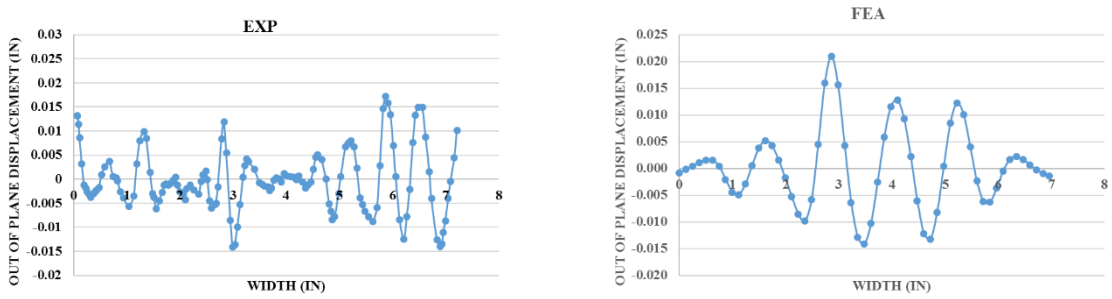

Figure 5.13: Experimental and simulation results of sample-3 at a load of 3 lbf

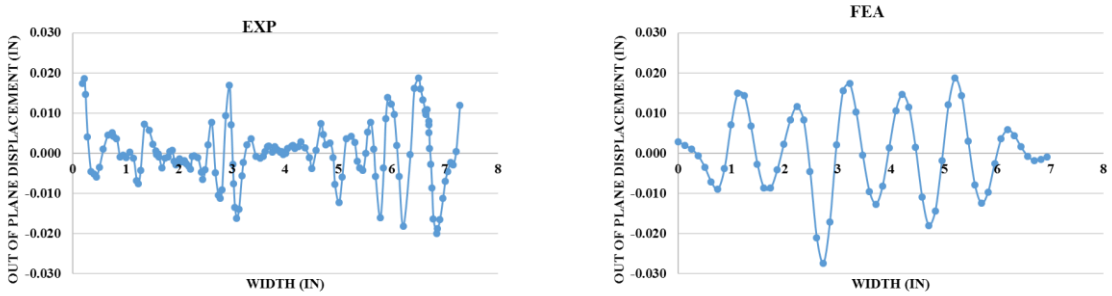

Figure 5.14: Experimental and simulation results of sample-3 at a load of 5 lbf

From the Figures 5.6-5.14, it is observed that:

- In some cases, the overall buckling amplitude agree reasonably well between FEA and experiments.
- the trough profile, especially the wavelength, of experimental data does not agree with simulation data. The trough profile all the three samples are different when compared with the simulation data.
- qualitatively some of the trough profiles are similar as the maximum amplitude of the trough profiles at respective load is same.

The differences in the trough profile possibly occur due to the following hypothesized factors:

1. In experimental trough profiles, curls are formed at edges when the load is applied. The SMS nonwoven web used in these experiments is a tri-layer structure that may have

induced asymmetric deformation in the out-of-plane direction, causing edge curling that affects the trough profile;

2. The orientation of loading cannot be controlled precisely in experiments, i.e., the web in MD should orthogonal to the clamps and the web in CMD should be parallel to the clamps. Due to the extremely small troughing load, sensitivity to loading imperfections can be a huge factor that alters the post-buckle trough profile.
3. Viscoelasticity properties of the web also affects the trough profile. During the experiment, when the load is applied and the displacement of the web is fixed, the web continues to deform and the load value starts to decrease. In order to see the difference, the web is loaded at certain load and the trough profile is recorded. The web is allowed to relax till the load reached a stationary value and the trough profile is recorded at that load.

   For example, a sample web of 23×7.5 in web is clamped at both ends to a Tensile Instron Machine to perform the trough profile test. A nonwoven web is clamped and stretched, and the trough profile is recorded right after the load reaches 5 lbf. Then, the web was allowed to relax until the load reaches a stagnant value, in this case, 3.85 lbf, and the trough profile is recorded again. The two recorded profiles are compared in Figure 5.15.

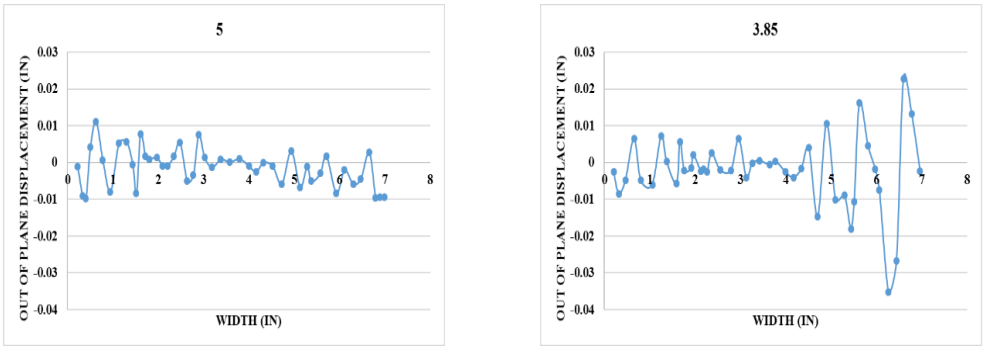

(a) (b)

Figure 5.15: Experimental trough profile of a nonwoven web (a) right after the application of 5 lbf, and (b) after the load is fully relaxed to 3.85 lbf

From the Figure 5.15, it can be clearly seen that the trough profiles are completely different in both amplitude and wavelengths. From this comparison, it appears that the nonwoven exhibits viscoelastic behavior. Future studies may need to eliminate these factors to better compare the FEA model with experiments.

In order to compare the trough profiles quantitatively, the amplitude and wavelength are calculated for 3 different samples as shown in Table 5.6 and 5.7 at different loads from trough profiles obtained from the experimental and finite element analysis.

Table 5.6: Comparison of Amplitude with FEA (non-uniform isotropic) results on nonwoven web

Load	web-1 (in)		web-2 (in)		web-3 (in)	
	FEA	EXP	FEA	EXP	FEA	EXP
1LB	0.0016	0.0037	0.004	0.0027	0.0025	0.0041
3LB	0.0095	0.0026	0.0141	0.035	0.0101	0.0056
5LB	0.0128	0.0036	0.0172	0.0043	0.0143	0.0054

Load	web-1 (in)		web-2 (in)		web-3 (in)		Average	
	FEA	EXP	FEA	EXP	FEA	EXP	FEA	EXP
1LB	1.263	0.248	1.261	0.341	1.419	0.277	1.314	0.29
3LB	1.144	0.202	1.229	0.252	1.169	0.442	1.18	0.30
5LB	1.043	0.281	0.991	0.254	0.991	0.27	1.008	0.27

Table 5.7: Comparison of Wavelength with FEA (non-uniform isotropic) results on nonwoven web

From Tables 5.6 and 5.7, it was observed that the average values of amplitudes and wavelengths of the experimental results differ largely with the experimental results.

POST-BUCKLING ANALYSIS -- UNIFORM ORTHOTROPIC MATERIAL:

The post buckling analysis of uniform orthotropic web is performed to analyze the troughs at a load of 1,3,5 lbf. The trough profile at the mid span of the web in MD along the CMD at different loads is shown in Figure 5.16-5.18. Here the trough only appears near the central 3 inches of the web, and these waves are used to calculate the wavelengths. The wavelengths of each trough profile is calculated and compared with experimental results at the end of this chapter.

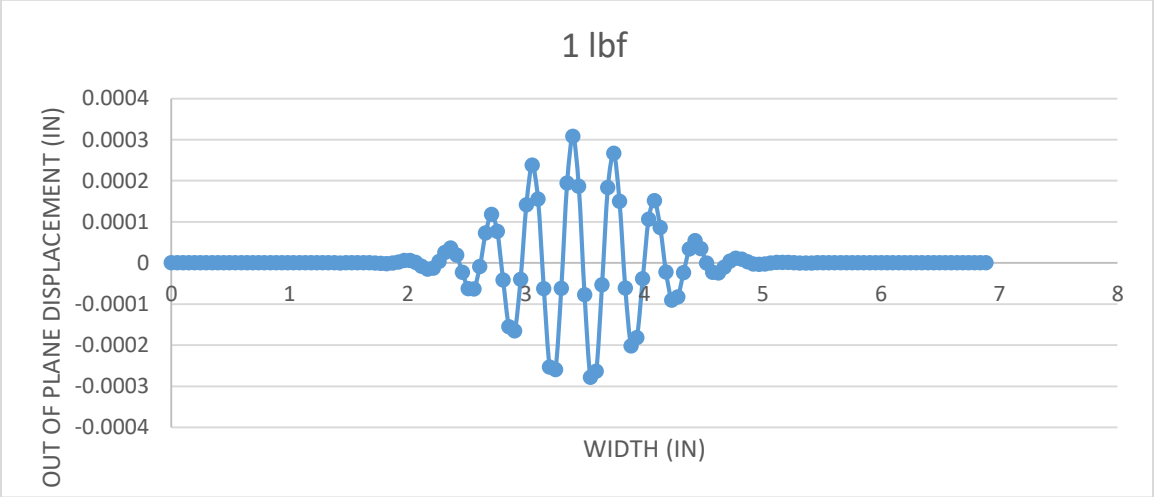

Figure 5.16: Trough profile at a load of 1 lbf

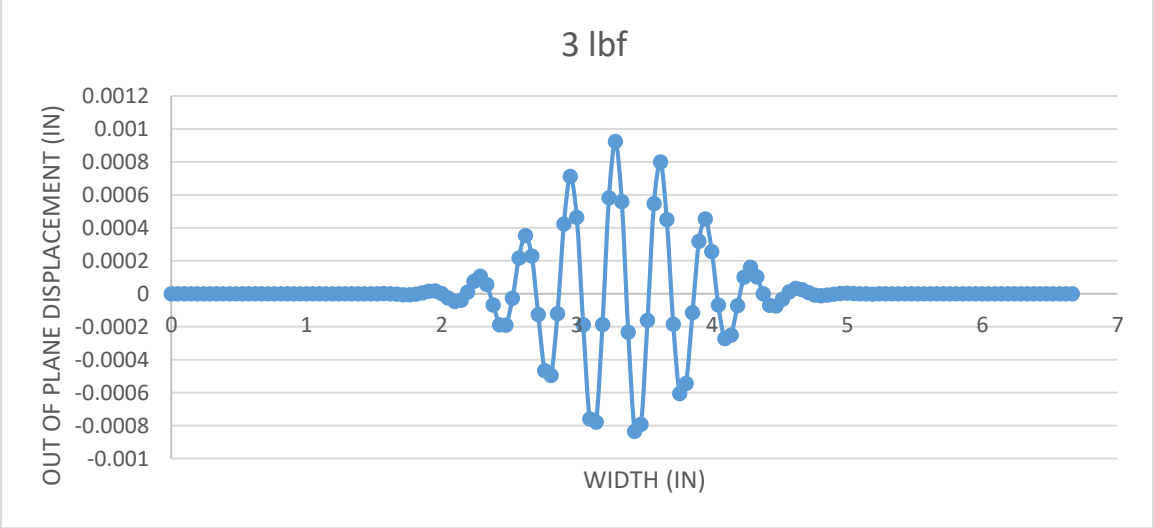

Figure 5.17: Trough profile at a load of 3 lbf

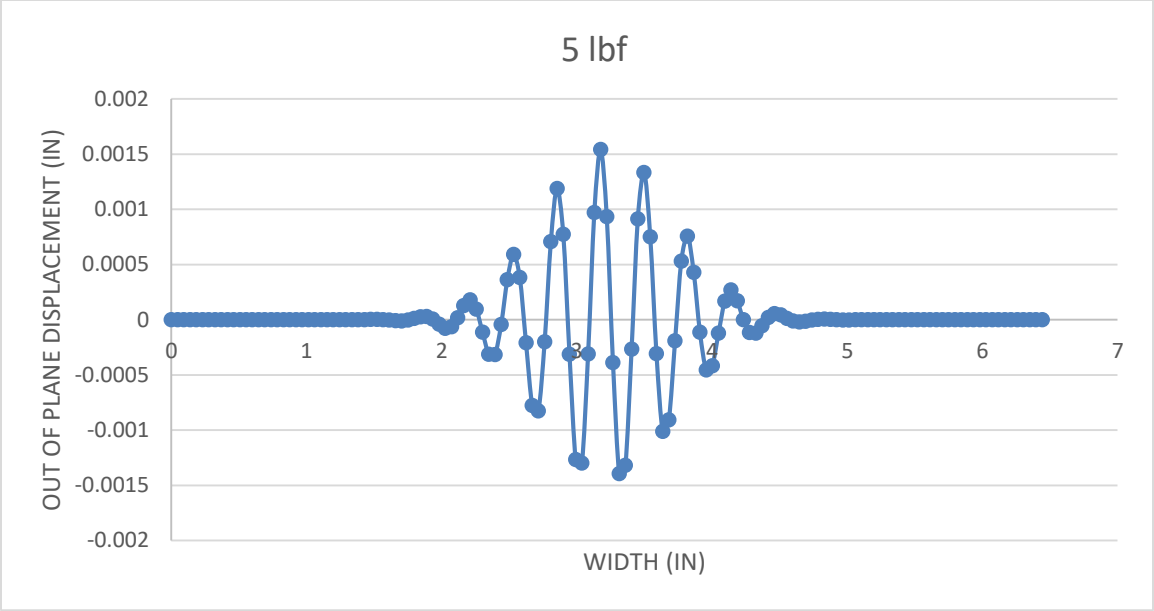

Figure 5.18: Trough profile at a load of 5 lbf

POST-BUCKLING ANALYSIS -- NON-UNIFORM ORTHOTROPIC MATERIAL:

The post-buckling analysis is performed on nonwoven web considered as orthotropic material (E_x and thickness from EA and thickness measurements, respectively, E_y assumed to be proportional to E_x) to analyze the troughs. This analysis is performed on three different webs at a load of 5 lbf. The trough profile at the mid span of the web in MD along the CMD can be obtained as the output. The trough profile data obtained from the FEA is compared with the experimental results to check the consistency of amplitude and wavelength. The troughs at a load of 5lbf is shown in Figure 5.19.

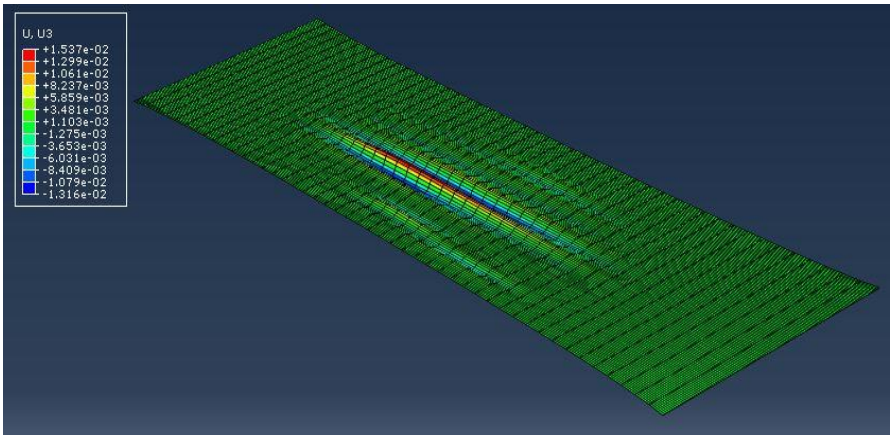

Figure 5.19: Troughs at a load of 5 lbf

The post-buckling analysis is carried out for non-uniform orthotropic materials at a load of 5lbf. The out of plane displacement data is obtained from this analysis. The data is plotted and compared with the trough profiles obtained from the experiment. Figure 5.16-5.18 shows the comparison of trough profile of different webs at a load of 5 lbf.

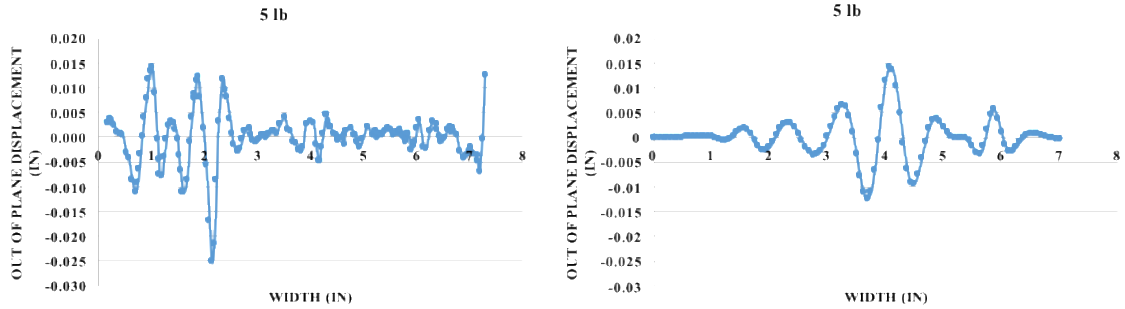

Figure 5.20: Experimental and simulation results of sample-1 at a load of 5 lbf

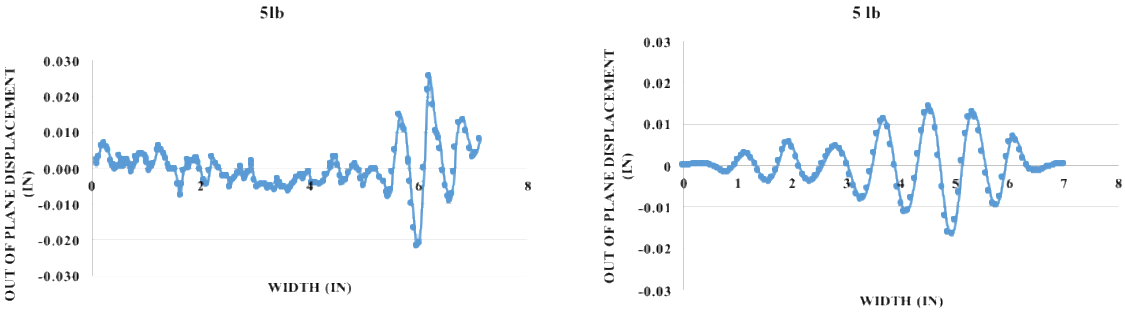

Figure 5.21: Experimental and simulation results of sample-2 at a load of 5 lbf

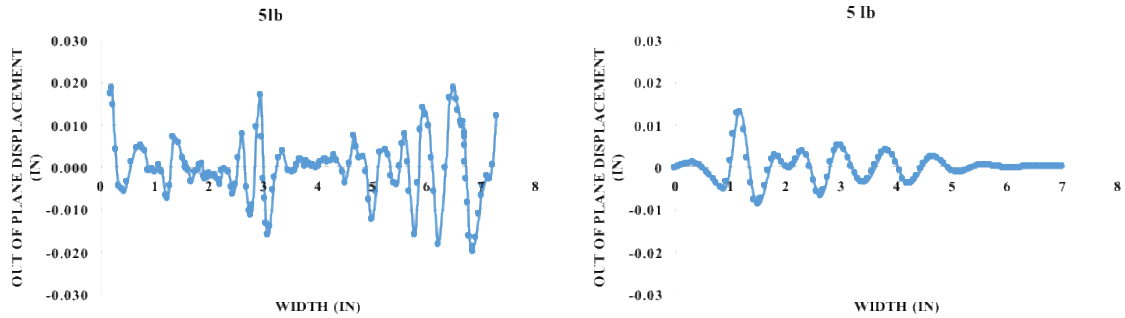

Figure 5.22: Experimental and simulation results of sample-3 at a load of 5 lbf

The wavelength and amplitude of SMS web considering it as non-uniform orthotropic is compared with experimental results and FEA results considering material as isotropic. The values are compared at a load of 5 lbf.

Table 5.8: Comparison of Amplitude with FEA results at load of 5 lbf

	Web -1	Web-2	Web-3
FEA (isotropic)	0.0128	0.0172	0.0143
FEA (non-uniform orthotropic)	0.005	0.0065	0.0049
Experimental	0.0036	0.0043	0.0054

Table 5.9: Comparison of Wavelength with FEA results at load of 5 lbf

	Web -1	Web-2	Web-3
FEA (isotropic)	1.043	0.991	0.991
FEA (non-uniform orthotropic)	0.729	0.822	0.7
Experimental	0.281	0.254	0.27

It can be seen from Tables 5.8-5.9 that considering the orthotropic properties of the web yields improved predictions of trough wavelengths.

COMPARISON OF EXPERIMENTAL WAVELENGTH RESULTS WITH FEA AND THEORETICAL RESULTS:

The wavelength of a uniform orthotropic web is calculated by using equation (2.10). The modulus E_y and poisons ratio of nonwovens are considered from Good and Beisel [4].

The parameters used in the equation are:

Table 5.10: Parameters used for wavelength calculation

σ_x	Length 'a' (in)	Width 'b' (in)	E_y (psi)	Thickness (in)	Poisson's ratio ν_{xy}	Poisson's Ratio ν_{yx}
calculated for different loads	23	7	1200	0.0047	0.3	0.04

The wavelength calculated at different loads using the above parameters is compared with the experimental results and FEA results considering material as uniform orthotropic. The wavelength from equation (2.10) compare well with the experimental and FEA results.

Table 5.11: Comparison of wavelengths

Comparison of wavelength (in)			
Load (lbf)	Good [4]	FEA (uniform orthotropic)	Experiment average
1	0.39	0.34	0.29
3	0.3	0.33	0.3
5	0.27	0.32	0.27

Theoretical prediction, FEA, and experiments agree very well.

CHAPTER VI

CONCLUSION AND RECOMMENDATIONS FOR FUTURE WORK

1. The studies using the ultrasonic thickness scanning and the resonance bending tests are not very successful due to the uncertainties in the measurements on thickness, tensile and bending stiffness. There are also factors such as the grid size, web thickness normalization, stiffness testing specimen sizes, etc. that are chosen by trial and error methods, which may be the source of inconsistencies between analysis and experimental results. A more rigorous study based on statistics methods should be performed to design better experiments to measure the property variations and define the sample sizes used in the analyses. Due to these reasons, most of the conclusions drawn from this study are hypotheses about what may work better for future studies.

2. The measurement in the tensile stiffness and the bending stiffness measurements have a number of sources for errors including what specimen sizes are chosen, how well the specimens are cut, and the averaging method (e.g. values for 4.5 mil samples are measured by taking samples that have thicknesses ranging from 4.46 to 4.54 mil). Much better material characterization methods need to be identified for future studies.

3. Orthotropic properties of the SMS nonwoven play an important role based on the study on buckling loads, as can be seen by the improved agreement between the orthotropic FE models and

experiments. Taking into account the orthotropic material properties of the SMS web are an important direction for future studies. Particularly, the CMD material properties need to be experimentally determined and fully studied.

4. Observations on post-buckling profiles indicate stress relaxation of the web under constant applied strain (stretch), which is a factor that needs to be considered after the problems mentioned in 1~3 are solved.

5. Codes are developed for implementing experimentally measured values of thickness and material property (isotropic or orthotropic) maps into ABAQUS input files that can be used in 2D plane-stress or 3D buckling/post-buckling finite element analyses. These codes are useful for future studies and can be adapted to account for other material behaviors when needed.

6. The wavelengths obtained from the experimental tests agree with both the FEA considering nonwoven web as a uniform orthotropic material and the wavelength predicted by the theoretical model by Good and Beisel [4], [5] using equation (2.10). The test results for wavelength appear to be valid.

REFERENCES

1) Bending stiffness of the paper and paperboard, TAPPI T 535 om-96.
2) V. Nukala, "Buckling of isotropic and orthotropic webs," MS Thesis, Oklahoma State University, 2016.
3) Beisel, J.A. and Good, J.K., The Instability of webs in transport, ASME Journal of Applied Mechanics, V78, 011001-1-7, January 2011.
4) J. K. GOOD and J. A. Beisel, "Calculations relating to web buckling resulting from roller misalignment," *TAPPI J.*, vol. 5, p. 8, 2006.
5) J.K. Good, J.A. Beisel, H. Yurtcu., Instability of webs: The prediction of troughs and wrinkles, Stillwater, Oxford, 2009, Vol. 1.
6) S.P. Timoshenko, J. M. Gere., Theory of Elastic Stability, Second Edition, New York, McGrawHill, 1961, p. 348
7) S. G. Baipa, "Wrinkling analysis on webs with circular non-uniform regions using finite elements," MS Thesis, Oklahoma State University, 2010.
8) S. Mallya, "Investigation of the effect of Voids on the Stability of Webs," MS Thesis, Oklahoma State University, 2007.
9) H. S. Yurtucu, "Development of nonlinear finite element codes for stability studies of web material with strain state dependent properties," MS Thesis, Oklahoma State University, 2011.
10) S. Timoshenko, Vibration Problems in Engineering: Read Books, 2009.
11) J.A. Biesel and J.K. Good, Buckling of orthotropic webs in process machinery.

12) E. Cerda, L. Mahadevan, Geometry and Physics of Wrinkling, UK: The American Physical Society, 2003.

13) Aswin Reddy, Ability of winding models to predict the length of the web material in a roll, MS Thesis, Oklahoma State University, 2016.

APPENDICES

```
import csv
import numpy as np
colt=168 #total number of columns
lim=np.linspace(1,24.0,96)      #start pos, end pos, number of positions
heat = [[0]*(colt//3) for _ in range(len(lim)-1)]
heati = [[0]*(colt//3) for _ in range(len(lim)-1)]
heatavg = [[0]*(56) for _ in range(len(lim)-1)]
rstart=3 #starting line of data
with open('density.csv', newline='') as ff:

        for x in range(1,len(lim)):
                spamreader = csv.reader(ff, dialect='excel', delimiter=',')
                ff.seek(0)
                rowi=0
                for row in spamreader:
                        rowi=rowi+1
                        if rowi>(rstart-1):
                                col=0
                                while(col<colt):
                                        #print(row[col+1])
                                        #input()
                                        #if (float(row[col+1])<60):
                                        #       col=col+3
                                        if (row[col]==""):
                                                col+=3
                                        elif (float(row[col])>lim[x-1] and float(row[col])<=lim[x]):
                                                heat[x-1][col//3]=heat[x-1][col//3]+float(row[col+1])
                                                heati[x-1][col//3]=heati[x-1][col//3]+1
                                                col=col+3
                                        else: col=col+3

                for yy in range(colt//3):
                        heat[x-1][yy]=heat[x-1][yy]/heati[x-1][yy]

for yy in range(56):
        for xx in range (92):
                for i in range(1):
                        heatavg[xx][yy]+=heat[xx][yy*1+i]/1

with open('output-density.csv','w',newline='') as ofile:
        spamwriter=csv.writer(ofile)
        spamwriter.writerows(heatavg)
```

Figure A.1: Python code to find the average thickness for different grid sizes

```
a=23
b=7
ngx=14
ngy=23
nex=10
ney=5
nx=ngx*nex
ny=ngy*ney

xsp=a/nx
ysp=b/ny
f=open('web.inp','w+')
f.write('*Preprint, echo=NO, model=NO, history=NO, contact=NO\n')
f.write('*Part, name=Part-1\n*End Part\n*Assembly, name=a\n*Instance,name=b,part=part-1\n')
f.write('*node\n')
#write nodes
nid=0
for row in range(ny+1):
    for col in range(nx+1):
        nid+=1
        f.write(str(nid)+',\t'+ str(xsp*col)+',\t'+ str(ysp*row)+'\n')

#write elements
f.write('*Element, type=CPS4R\n')
for row in range(ny):
    for col in range(nx):
        eid=row*nx+col+1
        f.write(str(eid)+',\t'+ str(row*(nx+1)+col+1)+',\t'+ str(row*(nx+1)+col+2)+
                ',\t'+ str((row+1)*(nx+1)+col+2)+',\t'+ str((row+1)*(nx+1)+col+1)+'\n')

#write node sets:
f.write('*Nset, nset=point\n1, '+str(1)+'\n')
f.write('*Nset, nset=Ledge, generate\n1, '+str(1+(nx+1)*ny)+', '+str(nx+1)+'\n')
f.write('*Nset, nset=Redge, generate\n'+str(nx+1)+', '+str((nx+1)*(ny+1))+
        ', '+str(nx+1)+'\n')
#import os
#write element sets:
for row in range(ngy):
    for col in range(ngx):
        f.write('*Elset, elset=elset'+str(row*ngx+col+1)+'\n')
        for ry in range(ney):
           for rx in range(nex):
              f.write(str(nx*(row*ney+ry)+col*nex+rx+1)+',')
           f.write('\n')
#f.seek(-1, os.SEEK_CUR)
f.write('\n')
```

FigureA.2: Python code for simulation of isotropic material

```
        ', '+str(nx+1)+'\n')
#import os
#write element sets:
for row in range(ngy):
    for col in range(ngx):
        f.write('*Elset, elset=elset'+str(row*ngx+col+1)+'\n')
        for ry in range(ney):
           for rx in range(nex):
              f.write(str(nx*(row*ney+ry)+col*nex+rx+1)+',')
           f.write('\n')
#f.seek(-1, os.SEEK_CUR)
f.write('*Orientation, name=Ori-1\n 1., 0., 0., 0., 1., 0.\n 3, 0.\n')

f.write('**Section\n')
import csv
import math
setid=0
with open(inputt, newline='') as ff:
            spamreader = csv.reader(ff, dialect='excel', delimiter=',')
            for row in spamreader:
                for kk in row:
                    setid=setid+1
                    #print(tij)
                    f.write('*Solid Section, elset=elset'+str(setid)+', material=Mater'+str(setid)+',orientation=Ori-1\n'+str(float(kk)/.0045*.0047)+', 5\n')#grid thickness here
                #print(row)

f.write('*end instance\n')
f.write('*Nset, nset=point,instance=b\n1, '+str(1)+'\n')
f.write('*Nset, nset=Ledge, instance=b,generate\n1, '+str(1+(nx+1)*ny)+', '+str(nx+1)+'\n')
f.write('*Nset, nset=Redge, instance=b, generate\n'+str(nx+1)+', '+str((nx+1)*(ny+1))+
        ', '+str(nx+1)+'\n')
f.write('*end assembly\n')
#write materials
import csv
import math
setid=0
with open(inputt, newline='') as ff:
            spamreader = csv.reader(ff, dialect='excel', delimiter=',')
            for row in spamreader:
                for kk in row:
                    setid=setid+1
                    t=float(kk)*100000
                    e1=0
                    if t<440:
                        e1=.1646*t-45.723
                    elif t>460:
                        e1=.0844*t-12.994
                    else: e1=-.0562*t+51.93
                    e1=e1/(t/450*.0047)/.5
                    e2=e1*8.27/55.1
                    f.write('*Material, name=Mater'+str(setid)+'\n*Elastic,type=LAMINA\n'+str(e1)+','+str(e2)+',0.48,'+str(e1/2./1.48)+','+str(e1/2./1.48)+','+str(e2/2./1.48)+'\n')#grid modulus here
                #print(row)
#write boundary conditions:
#f.write('*Boundary\npoint,1,2\n')
f.write('*Boundary\nLedge,1,2\n')
f.write('*Boundary\nRedge,2,2\n')
#write steps
#f.write('*Step, name=Step-1, nlgeom=NO\n*Static\n1., 1., 1e-05, 1.\n')
f.write('*Step, name=Step-1, nlgeom=NO\n*static\n1, 1.,1e-5 ,1\n')
#write loads
f.write('*Boundary\nRedge, 1, 1, 1\n') #load here
```

FigureA.3: Python code for meshing of non-uniform orthotropic material

```
#.25 by 1
a=23
b=7
ngx=23
ngy=28
nex=2
ney=4
f=open('w3buckle_025by1o.inp','w+')
inputt='./web3/0.25X1.csv'

"""
#.5 by 3
a=21
b=7
ngx=7
ngy=14
nex=12
ney=2
f=open('buckle_05by3.inp','w+')
inputt='./web1/0.5X3.csv'
"""
nx=ngx*nex
ny=ngy*ney
xsp=a/nx
ysp=b/ny
f.write('*Preprint, echo=NO, model=NO, history=NO, contact=NO\n')
f.write('*Part, name=Part-1\n*End Part\n*Assembly, name=a\n*Instance,name=b,part=part-1\n')
f.write('*node\n')
#write nodes
nid=0
for row in range(ny+1):
    for col in range(nx+1):
        nid+=1
        f.write(str(nid)+',\t'+ str(xsp*col)+',\t'+ str(ysp*row)+',\t0.\n')

#write elements
f.write('*Element, type=S4R\n')
for row in range(ny):
    for col in range(nx):
        eid=row*nx+col+1
        f.write(str(eid)+',\t'+ str(row*(nx+1)+col+1)+',\t'+ str(row*(nx+1)+col+2)+
                ',\t'+ str((row+1)*(nx+1)+col+2)+',\t'+ str((row+1)*(nx+1)+col+1)+'\n')

#write node sets:
f.write('*Nset, nset=point\n1, '+str(1)+'\n')
f.write('*Nset, nset=Ledge, generate\n1, '+str(1+(nx+1)*ny)+', '+str(nx+1)+'\n')
f.write('*Nset, nset=Redge, generate\n'+str(nx+1)+', '+str((nx+1)*(ny+1))+
        ', '+str(nx+1)+'\n')
#import os
#write element sets:
for row in range(ngy):
    for col in range(ngx):
        f.write('*Elset, elset=elset'+str(row*ngx+col+1)+'\n')
        for ry in range(ney):
           for rx in range(nex):
              f.write(str(nx*(row*ney+ry)+col*nex+rx+1)+',')
           f.write('\n')
#f.seek(-1, os.SEEK_CUR)
#f.write('*Orientation, name=Ori-1\n 1., 0., 0., 0., 1., 0.\n 3, 0.\n')

f.write('**Section\n')
import csv
import math
```

FigureA.4: Python code for buckling analysis of non-uniform orthotropic material

VITA

PHANIDHAR CHILUKA

Candidate for the Degree of

Master of Science

Thesis: EFFECTS OF NON-UNIFORMITY ON TROUGH INSTABILITY IN NONWOVENS

Major Field: MECHANICAL AND AEROSPACE ENGINEERING

Biographical:

Education:

Completed the requirements for the Master of Science in Mechanical and Aerospace Engineering at Oklahoma State University, Stillwater, Oklahoma in December, 2018.

Completed the requirements for the Bachelor of Technology in Mechanical Engineering at Osmania University, Hyderabad, Telangana, India in 2015.